

# HOTSPOTS, MANTLE PLUMES, FLOOD BASALTS, AND TRUE POLAR WANDER

R. A. Duncan  
*College of Oceanography*  
*Oregon State University, Corvallis*

M. A. Richards  
*Department of Geology*  
*University of California, Berkeley*

**Abstract.** Persistent, long-lived, stationary sites of excessive mantle melting are called hotspots. Hotspots leave volcanic trails on lithospheric plates passing across them. The global constellation of fixed hotspots thus forms a convenient frame of reference for plate motions, through the orientations and age distributions of volcanic trails left by these melting anomalies. Hotspots appear to be maintained by whole-mantle convection, in the form of upward flow through narrow plumes. Evidence suggests that plumes are deflected little by horizontal flow of the upper mantle. Mantle plumes are largely thermal features and arise from a thermal boundary layer, most likely the mantle layer just above the core-mantle boundary. Experiments and theory show that gravitational instability drives flow, beginning with the formation of diapirs. Such a diapir will grow as it rises, fed by flow through the trailing conduit and entrainment of surrounding mantle. The structure thus develops a large, spherical plume head and a long, narrow tail. On arrival at the base of the

lithosphere the plume head flattens and melts by decompression, producing enormous quantities of magma which erupt in a short period. These are flood basalt events that have occurred on continents and in ocean basins and that signal the beginning of major hotspot tracks. The plume-supported hotspot reference frame is fixed in the steady state convective flow of the mantle and is independent of the core-generated (axial dipole) paleomagnetic reference frame. Comparison of plate motions measured in the two frames reveals small but systematic differences that indicate whole-mantle motion relative to the Earth's spin axis. This is termed true polar wander and has amounted to some 12° since early Tertiary time. The direction and magnitude of true polar wander have varied sporadically through the Mesozoic, probably in response to major changes in plate motions (particularly subduction zone location) that change the planet's moments of inertia.

---

## 1. INTRODUCTION

The plate tectonics model has been largely successful in explaining the distribution of basaltic volcanism on our planet. Mid-ocean ridge basalts are produced by decompression melting of passively upwelling upper mantle (asthenosphere) at the edges of separating plates, while subduction of oceanic lithosphere causes upper mantle hydration and melting, yielding volcanic arc basalts along collisional plate boundaries. Such plate margin environments account for the vast majority of all magma production. A volumetrically minor but significant class of basaltic volcanism occurs within plates or crosses plate boundaries, and it is characterized by linear chains of volcanoes (hotspot lineaments) that grow older in the directions of plate motion. Classic examples of this volcanic phenomenon are the Hawaiian Islands (and other parallel island chains in the Pacific Ocean), the Yellowstone-Snake River Plain province, and the volcanic platform and ridge system centered on Iceland. Because of

their geometry and age distributions these volcanic provinces are thought to result from focused upper mantle zones of melting called hotspots [Wilson, 1963, 1965] that remain stationary as the Earth's outer shell of lithospheric plates move across them. The proposed locations of present hotspot volcanism are shown in Figure 1.

Morgan [1971, 1972] proposed that hotspots are maintained by unusually warm material rising from the lower mantle through narrow conduits that he called mantle plumes. He further speculated that these plumes comprised the upward flow of a long-lived, stable pattern of whole-mantle convection (Figure 2). Once established, these conduits for heat and material transport from the lower mantle do not, Morgan proposed, change position relative to one another. Plumes probably initiate in the seismically defined thermal layer at the boundary between the core and mantle. Convection in the lower mantle is likely to be very sluggish [Gurnis and Davies, 1986] so plumes rising through this region should not be "deflected," or drift with respect to one another. Convec-



this field acquire a magnetic inclination (angle of the rock magnetic vector from horizontal) unique to their latitude. Thus any translational (north-south) motion of lithospheric plates can be determined from the paleomagnetic reference frame; east-west motions are not found by this method. Comparison of plate motions deduced from the hotspot and paleomagnetic reference frames indicates a small shift of the whole mantle with respect to the Earth's spin axis since early Tertiary time (55–65 Ma).

In this paper we review the evidence for interhotspot motion and examine the question of whether hotspot lineaments constitute a useful frame of reference for plate motions. This issue also pertains to the geometry and dynamics of convective flow in the mantle, which in turn constrain estimates of the viscosity structure of the mantle. Many hotspots appear to have begun with massive outpourings of basaltic magmas over broad regions, both on continents and in ocean basins. These volcanic provinces are called flood basalts and probably mark the arrival and initial melting of the "heads" of mantle plumes at the base of the lithosphere. Subsequent volcanism over the plume conduits (or "tails"), established by the initial plume upwelling, are the familiar tracks that connect flood basalts to presently active hotspots.

## 2. ARE HOTSPOTS STATIONARY?

An important question concerning hotspot volcanism is whether or not mantle plumes are, in fact, fixed with respect to one another and thus define an irregular but rigid reference frame. Some amount of interplume (hotspot) motion might be expected because of viscous coupling between the base of the moving lithospheric plates and the upper mantle owing to horizontal flow of the upper mantle away from spreading centers (Figure 2). If these perturbations are small or constant over long periods, then interplume drift may be significantly less than plate velocities, and hotspots with associated volcanic traces constitute a convenient and direct reference frame for reconstructing plate motions, independent of the paleomagnetic reference frame.

The magnitude of interplume motion can be assessed by comparing the geometry and age distribution of volcanism along hotspot tracks with past plate movements reconstructed from relative motion data. If the motion of one plate over hotspots underlying it is determined from the orientation and age of volcanism along trails of islands, seamounts, and linear ridges, reconstructions of the past positions of neighboring plates with respect to those hotspots can be calculated from seafloor spreading data. If hotspots underlying all plates are stationary, then the calculated motions of the neighboring plates should follow hotspot tracks observed on them. Any deviations of these predicted plate movements from actual hotspot tracks would then indicate the magnitude and direction of interplume drift.

*Morgan* [1972] first noted the congruence of the major island and seamount chains on the largest and fastest-moving Pacific plate (Hawaiian-Emperor, Tuamotu-Line, and Austral-Gilbert-Marshall island and seamount lineaments). The geometry of these volcanic traces can be reasonably well matched by rigid plate motion over hotspots fixed at the present locations of Hawaii, Easter Island, and Macdonald Seamount, respectively. Subsequent studies, incorporating the distribution of the age of volcanism as well as the geometry of the traces [*Clague and Jarrard*, 1973; *Jarrard and Clague*, 1977; *Duncan and McDougall*, 1976; *McDougall and Duncan*, 1980; *Duncan and Clague*, 1985; *Lonsdale*, 1988], have confirmed the fixed positions of Pacific hotspots over the past 65 m.y. *Morgan* [1981] and *Duncan* [1981] showed that a similar case can be made for rigid motion of the African plate over a fixed set of hotspots underlying the central and South Atlantic and western Indian ocean basins since 120 Ma (Figure 3).

*Minster et al.* [1974] and *Minster and Jordan* [1978] found no detectable interhotspot movement for the past 5–10 m.y., on the basis of a best fitting global set of relative plate motions tied to Pacific hotspots. Early comparisons of Atlantic with Indian and Pacific Ocean hotspots, on the other hand, reported relative motions of hotspots up to 10–20 mm/yr during Tertiary time [*Burke et al.*, 1973; *Molnar and Atwater*, 1973; *Molnar and Francheteau*, 1975]. However, improved relative plate motion information and better age resolution of the older ends of hotspot traces led *Morgan* [1981, 1983] and *Duncan* [1981] to conclude that movement between North Atlantic and Indian Ocean hotspots must be less than 5 mm/yr. *Molnar and Stock* [1987] have recently revived this debate by proposing that the Hawaiian hotspot has moved southward 10–20 mm/yr (km/m.y.) with respect to hotspot traces in the Atlantic and Indian oceans. By starting with the Pacific plate hotspot traces, however, all plate circuits to plates bordering the Indian or Atlantic oceans must include Antarctica. *Molnar and Stock* [1987, p. 587] specifically "neglect deformation between East and West Antarctica." This contradicts paleomagnetic evidence that East and West Antarctica have experienced differential rotations since the Early Cretaceous [*Watts and Bramall*, 1981; *Mitchell et al.*, 1986; *Martin*, 1986] accommodated by a proposed plate boundary through the Ross Sea–Weddell Sea region during Cenozoic time [*Molnar et al.*, 1975; *Gordon and Cox*, 1980; *Stock and Molnar*, 1982; *Jurdy*, 1979; *Duncan*, 1981]. Identification of a small oceanic plate in the Bellinghousen Sea [*Stock and Molnar*, 1987] now requires significantly less motion between Pacific and other hotspots (5–10 mm/yr (J. Stock, personal communication, 1990)).

A far less ambiguous test of hotspot fixity is to compare Atlantic and Indian Ocean hotspot positions through time (because all intervening plate boundaries are divergent and relative motions are recorded accurately on the seafloor). Since the *Morgan* [1981, 1983] and *Duncan* [1981]

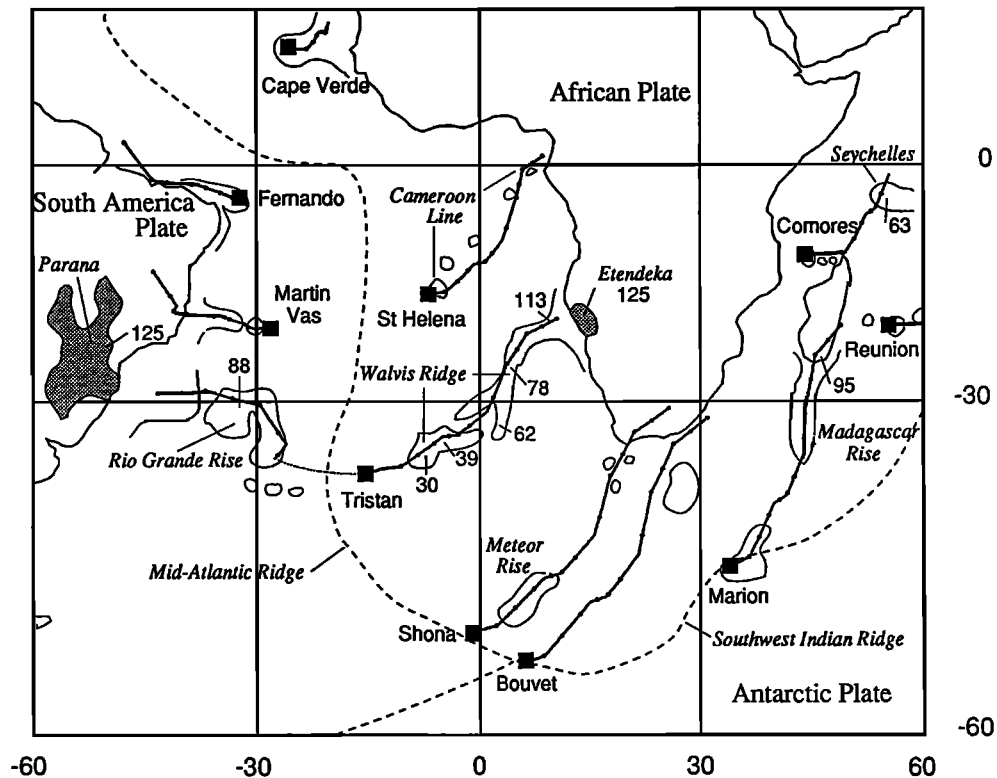


**Figure 3.** Modeled hotspot tracks for the southern Atlantic Ocean basin. (The ages, in millions of years, of radiometrically dated locations are indicated, while solid dots along tracks are 10-m.y. increments of predicted volcano age.) Rotation parameters are chosen by trial and error to fit simultaneously the geometry and age progression of volcanism along hotspot tracks on the African plate (Walvis Ridge, Cameroon line, Madagascar

Ridge, and Mascarene Plateau lineaments). Relative plate motions are added to obtain predicted hotspot tracks on neighboring plates, assuming fixed hotspots. The generally excellent match between predicted and observed tracks supports the idea that hotspots move very slowly (2–5 mm/yr), if at all. The Parana-Etendeka flood basalts attending the birth of the Tristan hotspot are stippled.

analyses, there have been several revisions in relative plate motions, and the volcanic histories of many prominent hotspot traces have been resolved. Hence a more definitive examination of interhotspot motions can now be made, and a revised set of plate rotations appears in Table 1.

Figure 3 illustrates the rotation parameters for motion of the African plate over stationary hotspots since 120 Ma (the time of continental breakup in the South Atlantic), on the basis of the geometry and radiometric ages for the Walvis Ridge and Cameroon Line [O'Connor and Duncan, 1990; O'Connor, 1990]. As noted by earlier studies, the hotspot traces can be matched by rigid plate motion over a set of fixed hotspots distributed over  $100^\circ$  (11,000 km) of the Earth's surface. Now that the age of volcanism along the Walvis Ridge is known in detail (from reliable  $^{40}\text{Ar}$ – $^{39}\text{Ar}$  incremental heating experiments on dredged and cored volcanic samples), rates of plate motion can be assigned for time intervals with more precision, especially for the period 30–80 Ma. Similarly dated samples from the Cameroon Line [O'Connor, 1990], the Marion-Madagascar track (R. A. Duncan, unpublished data, 1990), and the Réunion-Mascarene track [Duncan and Hargraves, 1990] corroborate these angular velocities. The geometry

of the Shona Ridge–Meteor Rise track [Hartnady and Roex, 1985] is in accord with a stationary hotspot. Hence these linear volcanic tracks across the entire African plate are compatible with fixed hotspots, during the past 120 m.y.

South and North American plate motions over the hotspot network are calculated by adding the latest relative plate motions [Cande et al., 1988; Klitgord and Schouten, 1985] to the motion of the African plate over hotspots (Figures 3 and 4). Hotspot traces predicted from these plate rotations can then be compared with volcanic lineaments associated with Atlantic hotspots to check further the fixed hotspot hypothesis. The most prominent and long-lived hotspot traces are the Rio Grande Rise (South Atlantic, Figure 3) and the New England Seamounts (North Atlantic, Figure 4). The geometry and few dated positions along the Rio Grande Rise [O'Connor and Duncan, 1990] are matched by the calculated rotations. The Tristan da Cunha hotspot generated the Rio Grande Rise simultaneously with the eastern half of the Walvis Ridge, when the South Atlantic spreading ridge lay centered over the hotspot. From about 70 to 50 Ma the spreading ridge migrated westward in a series of jumps to its present posi-

TABLE 1. Plate Rotations in the Hotspot Reference Frame, 120 Ma to Present

| Period, Ma                  | Total Rotations, deg |                |               | Period, Ma                        | Total Rotations, deg |                |               |
|-----------------------------|----------------------|----------------|---------------|-----------------------------------|----------------------|----------------|---------------|
|                             | Latitude (+N)        | Longitude (+E) | Angle (+CCW)* |                                   | Latitude (+N)        | Longitude (+E) | Angle (+CCW)* |
| <i>African Plate</i>        |                      |                |               | <i>Eurasian Plate (continued)</i> |                      |                |               |
| 11-0 (A5)†                  | 60.0                 | -30.0          | -2.0          | 58-0                              | 7.6                  | -46.2          | -12.4         |
| 21-0 (A6)                   | 51.0                 | -45.0          | -4.5          | 66-0                              | 9.5                  | -44.6          | -16.0         |
| 36-0 (A13)                  | 40.0                 | -45.0          | -8.0          | 80-0                              | 11.0                 | -56.2          | -18.0         |
| 42-0 (A18)                  | 42.0                 | -42.5          | -9.0          | 100-0                             | 7.0                  | 107.0          | 17.8          |
| 48-0 (A21)                  | 42.0                 | -40.0          | -9.6          | 120-0                             | 27.5                 | 88.9           | 19.7          |
| 58-0 (A26)                  | 40.0                 | -40.0          | -10.7         | <i>Indian Plate</i>               |                      |                |               |
| 66-0 (A29)                  | 35.0                 | -40.0          | -14.5         | 11-0                              | 37.7                 | 26.7           | -6.4          |
| 80-0                        | 31.0                 | -50.0          | -20.0         | 21-0                              | 31.0                 | 27.6           | -12.7         |
| 100-0                       | 25.0                 | -47.0          | -25.5         | 36-0                              | 24.2                 | 26.4           | -21.8         |
| 120-0 (M0)                  | 26.0                 | -42.5          | -30.0         | 42-0                              | 26.4                 | 27.2           | -25.6         |
| <i>South American Plate</i> |                      |                |               | 48-0                              | 26.8                 | 24.2           | -29.6         |
| 11-0                        | 58.7                 | -45.3          | 2.1           | 58-0                              | 26.9                 | 13.5           | -36.4         |
| 21-0                        | 68.8                 | -13.5          | 3.3           | 66-0                              | 20.4                 | 10.3           | -48.6         |
| 36-0                        | 72.3                 | 13.5           | 6.4           | 80-0                              | 19.3                 | 2.8            | -62.5         |
| 42-0                        | 70.7                 | 3.1            | 7.6           | 100-0                             | 14.3                 | 6.6            | -70.7         |
| 48-0                        | 70.6                 | -6.0           | 10.3          | 120-0                             | 14.0                 | 3.7            | -77.0         |
| 58-0                        | 74.4                 | 0.1            | 13.0          | <i>Antarctic Plate</i>            |                      |                |               |
| 66-0                        | 78.0                 | 64.5           | 13.4          | 11-0                              | 57.1                 | -117.1         | -3.0          |
| 80-0                        | 66.2                 | 63.8           | 18.0          | 21-0                              | 74.5                 | -110.2         | -3.7          |
| 100-0                       | 62.1                 | 31.2           | 22.9          | 36-0                              | 72.7                 | -63.5          | -4.7          |
| 120-0                       | 56.1                 | 6.7            | 27.1          | 42-0                              | 85.9                 | -3.4           | -4.8          |
| <i>North American Plate</i> |                      |                |               | 48-0                              | 83.2                 | 136.4          | -6.4          |
| 11-0                        | 27.0                 | 128.2          | 1.4           | 58-0                              | 77.5                 | -113.5         | -10.2         |
| 21-0                        | 30.4                 | 113.2          | 3.3           | 66-0                              | 78.8                 | -16.9          | -10.1         |
| 36-0                        | 39.8                 | 108.9          | 6.7           | 80-0                              | 76.6                 | -152.4         | -14.1         |
| 42-0                        | 46.1                 | 111.2          | 7.8           | 100-0                             | 89.1                 | -52.7          | -15.5         |
| 48-0                        | 53.1                 | 113.1          | 9.4           | 120-0                             | 80.4                 | -169.4         | -22.4         |
| 58-0                        | 59.1                 | 112.3          | 12.6          | <i>Australian Plate</i>           |                      |                |               |
| 66-0                        | 50.3                 | 118.6          | 15.9          | 11-0                              | 25.9                 | 41.3           | -7.8          |
| 80-0                        | 49.3                 | 101.8          | 20.6          | 21-0                              | 20.1                 | 40.3           | -15.6         |
| 100-0                       | 58.4                 | 80.2           | 29.9          | 36-0                              | 17.7                 | 34.1           | -24.6         |
| 120-0                       | 62.3                 | 61.1           | 37.7          | 42-0                              | 20.3                 | 33.6           | -28.4         |
| <i>Eurasian Plate</i>       |                      |                |               | 48-0                              | 24.6                 | 33.1           | -28.0         |
| 11-0                        | 38.2                 | -47.2          | -2.7          | 58-0                              | 32.9                 | 23.1           | -27.5         |
| 21-0                        | 30.5                 | -55.7          | -5.3          | 66-0                              | 29.2                 | 23.7           | -29.5         |
| 36-0                        | 20.0                 | -60.4          | -8.4          | 80-0                              | 35.4                 | 28.1           | -28.2         |
| 42-0                        | 18.2                 | -55.9          | -9.3          | 100-0                             | 49.5                 | 26.8           | -32.1         |
| 48-0                        | 14.3                 | -52.0          | -10.0         | 120-0                             | 72.7                 | 28.1           | -39.5         |

\* CCW means counterclockwise.

† A5 etc. are the seafloor magnetic anomalies used in relative plate motion reconstructions.

tion 400 km west of the Tristan hotspot; this process eventually terminated the growth of the Rio Grande Rise at its eastern end. The Tristan hotspot was born at about 125 Ma with massive eruptions of flood basalts, now preserved at the western end of the Rio Grande Rise (the Parana basalts) and the eastern end of the Walvis Ridge (the Etendeka basalts), a point we will return to in the next section.

The New England Seamounts form a 1000-km-long, northwest-southeast trending chain of submarine volcanoes in the western central Atlantic basin. Radiometric dating ( $^{40}\text{Ar}$ - $^{39}\text{Ar}$  ages) has shown that the age of volcanism decreases smoothly from 103 to 82 Ma (southeastward) along the lineament [Duncan, 1984]. This volcanic trace continues eastward to the Corner Seamounts, whose ages

are estimated from subsidence calculations to be in the range of 80-70 Ma [Tucholke and Smoot, 1990]. Crough [1981] and Morgan [1983] proposed a hotspot position near Great Meteor Seamount in the eastern central Atlantic basin that was overridden (and hence separated from its track on the North American plate) by the Mid-Atlantic Ridge soon after the formation of the Corner Seamounts. Figure 4 compares the trace of the New England hotspot predicted from fixed hotspots with the position and age of volcanic structures in the central Atlantic basin. The close match in geometry and age of volcanism between predicted and observed traces is strong evidence that the New England hotspot has remained fixed with respect to hotspots in the South Atlantic since the beginning of Cretaceous time.

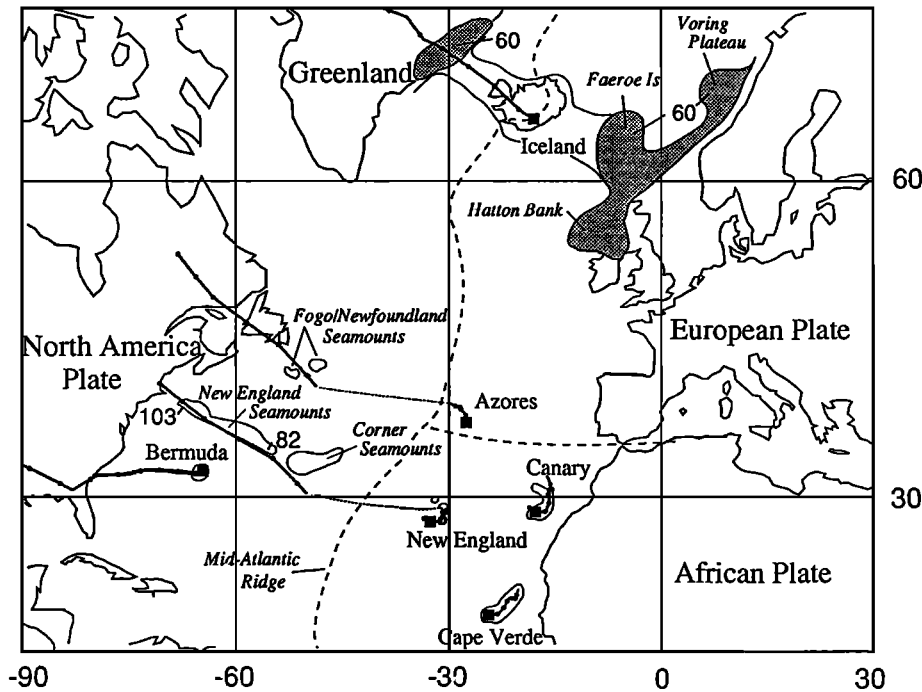


**Figure 4.** Modeled hotspot tracks for the northern Atlantic Ocean basin (see Figure 3 for details). The text discusses the volcanism attending the birth of the Iceland hotspot.

Calculated North American plate motion in the vicinity of the Iceland hotspot also agrees well with the orientation of the Iceland-Greenland Ridge, but not with the timing (60 Ma) of flood basalt volcanism along the east coast of Greenland, an observation noted by *Morgan* [1983] and *Vink* [1984]. Our modeling predicts that at 60 Ma the Iceland hotspot lay beneath central Greenland, some 600 km from the plate edge where the North Atlantic Tertiary Province flood basalts were erupted. This situation requires either that (1) the Iceland hotspot has drifted southeast at an average rate of 10 mm/yr relative to South Atlantic hotspots, or (2) during its initial eruptions at 60 Ma the hotspot was very large (~1000 km diameter, Figure 4) and could feed flood basalts to a region including the Hatton Bank, Vøring Plateau, and the Disko Basalts of western Greenland [*White and McKenzie*, 1989]. *Vink* [1984] presented a model in which a small-diameter hotspot under Greenland fed spreading ridge eruptions at the Vøring Plateau, eastern Greenland, and the Faeroes Plateau by horizontal asthenospheric flow until Greenland drifted away from the hotspot and ridge-centered volcanism was established. In view of the large region of flood basalt eruptions likely during a plume initiation event (see next section) we feel that the notion of a point source for the Iceland hotspot is not applicable at 60 Ma. Following the flood basalt event the hotspot probably decreased to "normal" size, and the predicted younger volcanic trail (50 Ma to present) follows the Iceland-Greenland and western Iceland-Faeroes ridges. We can conclude that hotspots throughout the Atlantic basin, from Marion and Réunion to the central Atlantic (and possibly Iceland), have remained fixed for at least the past 60 m.y., and the longer-lived

hotspots (New England, Tristan, Marion) show no detectable relative motion since 120 Ma.

Turning next to the Indian Ocean, Indian plate and Antarctic plate motions over hotspots are found by adding the latest appropriate relative plate motions [*Molnar et al.*, 1987; *Royer and Sandwell*, 1989] to the African plate over hotspots rotations. The *Royer and Sandwell* [1989] rotations incorporate a wealth of improved relative motion data for the Indian Ocean basin [*Patriat*, 1983]. The resulting Indian plate motions can then be compared with prominent volcanic traces emanating from the Réunion and Kerguelen hotspots (Figure 5). Recently, legs 115 and 121 of the Ocean Drilling Program focused on obtaining volcanic samples from these lineaments: the Mascarene-Chagos-Maldives Ridge (Réunion hotspot trace) and the Ninetyeast Ridge (Kerguelen hotspot trace). The age distribution of the volcanism along these trends is now well resolved by  $^{40}\text{Ar}$ - $^{39}\text{Ar}$  dating [*Duncan and Hargraves*, 1990; *Duncan*, 1978, 1991], so any departures from fixed hotspots should be easily identified.

Figure 5 shows predicted hotspot traces (which assume fixed hotspots) superimposed on actual volcanic structures found on the floor of the Indian Ocean basin. A very good match between predicted and observed traces is obtained by locating the Réunion hotspot beneath a large seamount 150 km to the west of the volcanically active island of Réunion, and the Kerguelen hotspot beneath a group of prominent seamounts on the northwest margin of the Kerguelen Plateau. Both hotspots began with flood basalt events (the Deccan Traps and the Rajmahal Traps, respectively; see also Figure 12), then left parallel, north to south growing volcanic ridges on the trailing edge of the

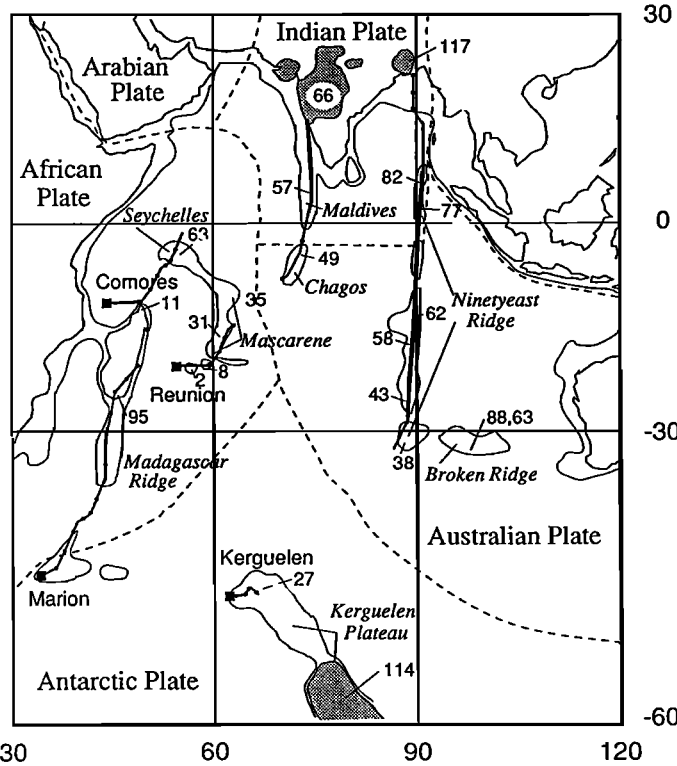


Figure 5. Modeled hotspot tracks for the Indian Ocean basin (see Figure 3 for details). Ages shown are radiometric age determinations for basalts from the two prominent volcanic lineaments: the Réunion and Kerguelen hotspot tracks. Flood basalt provinces (stippled) mark the initiation of each of these hotspots.

rapidly moving Indian plate and were overridden by the central and southeast Indian spreading ridge at 36–38 Ma. From that time forward the Réunion hotspot has formed the Mascarene Plateau and the islands of Mauritius and Réunion on the African plate, while the Kerguelen hotspot has formed a large part of the northern Kerguelen Plateau on the slowly moving Antarctic plate.

Finally, seamount chains in the Tasman Sea and continental basaltic volcanism in eastern Australia have been linked to hotspot activity [Vogt and Conolly, 1971]. Recent radiometric dating of the seamounts [McDougall and Duncan, 1988] has confirmed a north to south, monotonic age progression in the volcanism of the same rate as observed in chains of central volcanoes in eastern Australia for the past 35 m.y. [Wellman and McDougall, 1974]. This region lies in the easternmost part of the Indian plate. There is evidence from seismicity and geoid anomalies that an east-west plate boundary occurs within the central Indian basin which has allowed a small amount of north-south compression between the Indian plate and the Australian plate over the past 10 m.y. [Royer, 1988; DeMets et al., 1988; Stein et al., 1990]. This proposed relative plate motion has been incorporated in the predicted motion for the Australian plate, which closely matches the orientation and age progression of the Tasman seamount chain (Figure 6). Hotspot activity in the vicinity of the Antarctic Balleny Islands has left a volcanic trail on the Australian plate that shows up particularly well on geoid anomaly maps. A single dated seamount fits well with the predicted age of the trace southeast of Tasmania.

In summary, geometrical and age comparisons of volcanic chains with computer-generated traces calculated

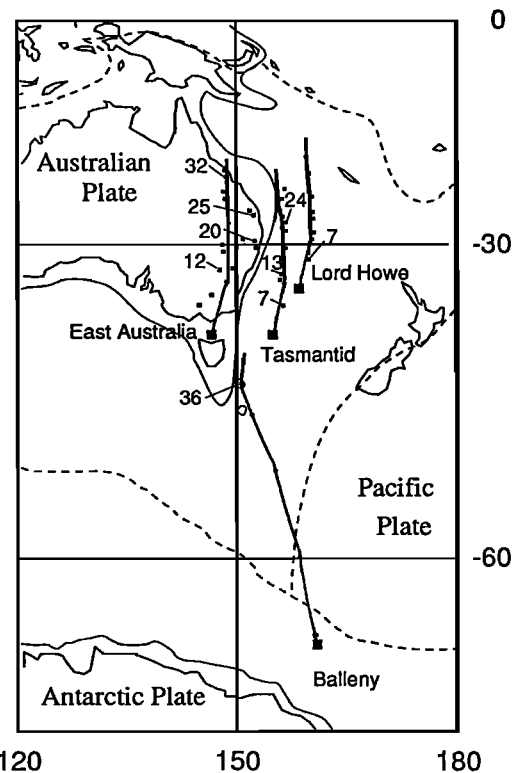


Figure 6. Modeled hotspot tracks for the eastern Australian plate (see Figure 3 for details). Ages shown are radiometric age determinations [McDougall and Duncan, 1988; R. A. Duncan, unpublished data for southeast Tasmania, 1990]. Solid squares are locations of volcanic centers.

by linking African plate motion over hotspots motion to neighboring plates demonstrates that there is no perceptible interhotspot motion over periods as long as 120 m.y. Moreover, the examined hotspots range from Iceland in the North Atlantic through the South Atlantic and Indian oceans to the Tasman sea, a region exceeding half the Earth's surface and including six major plates. According to *Molnar and Stock* [1987], 95% uncertainty ellipses for relative plate motion additions have typical semimajor axes of 200–300 km, so the maximum allowable relative motion among these hotspots is about 2–5 mm/yr. The real motion is thus at least an order of magnitude less than typical lithospheric plate velocities. There is no evidence for any systematic departure between modeled and observed hotspot traces from one plate to the next, which might be expected if hotspots are greatly affected by horizontal flow in the upper mantle. Over this half of the globe, then, hotspots are fixed to the extent that they constitute a stable reference frame for plate motions, recorded simply as volcanic trails.

Further extension of this analysis into the Pacific region is limited by subduction plate boundaries, where relative motion histories are largely destroyed, or the ice-covered Antarctic plate, where plate boundaries are poorly known. However, we know that Pacific basin hotspots have been stationary since 65 Ma [*Duncan and Clague*, 1985]. *Molnar and Stock's* [1987] conclusion that as much as 20 mm/yr interhotspot motion has occurred can thus have one of two explanations: either Pacific hotspots have moved (southward) en masse with respect to fixed hotspots in the Atlantic and Indian oceans, or all hotspots worldwide are fixed and there is some as yet poorly known plate boundary within the Antarctic plate that has accommodated relative motion during Cenozoic time. The second possibility appears to be more likely, and the required relative motion between East and West Antarctica can be calculated from the fixed hotspot reference frame [*Duncan*, 1981].

### 3. TRUE POLAR WANDER: DOES THE MANTLE ROLL?

If we now accept the conclusion of section 1 that mantle plumes are stationary, to within about 5 mm/yr or less, over periods as long as 120 m.y., then the volcanic traces left by hotspots record the histories of plate motions over the lower mantle. This mantle reference frame is independent of the paleomagnetic reference frame and has certain distinct advantages. It does not depend on the assumption of the geocentric axial dipole field (for which there is good evidence except during polarity reversals of the field), and it resolves east-west plate motion which is not detected in paleomagnetic studies. Several groups have used the mantle reference frame to determine the history of plate convergence across subduction zones, where the record of relative plate motion is largely

destroyed [*Engebretson et al.*, 1984, 1986; *Duncan and Hargraves*, 1984; *Rea and Duncan*, 1986; *Pollitz*, 1988]. Continental tectonic and volcanic events in western North America are particularly well correlated with changes in the magnitude and direction of plate convergence predicted from the hotspot reference frame [*Engebretson et al.*, 1984; *Wells et al.*, 1984; *Verplanck and Duncan*, 1987]. This method eliminates the need to construct global circuits of plate motions that cross only spreading ridges [*Jurdy*, 1984] and reduces the large uncertainties accumulated in combining sequences of rotation poles [*Molnar and Stock*, 1985].

Now, differential motion between the mantle and the spin axis can in principle be determined by comparing plate motions recorded by the hotspot and paleomagnetic reference frames. Such motion has been termed true polar wander (distinguished from apparent polar wander of the magnetic (spin) axis inferred from time sequences of paleomagnetic field directions for given plates). It is possible that redistribution of mass within the Earth through processes such as mantle convection and plate motions may change the planet's moments of inertia sufficiently to cause a shift of the entire body relative to its spin axis [*Goldreich and Toomre*, 1969]. This is, in fact, an old idea, suggested as an alternative to continental drift as an explanation for paleoclimatic evidence for translatitudinal motion of the Earth's surface [*Irving*, 1964]. True polar wander, however, was largely ignored after it was demonstrated that separate continents had distinct apparent polar wander paths and that continental drift (plate motions) must have occurred [e.g., *Runcorn*, 1965]. Could both motions occur simultaneously?

In the absence of true polar wander, mantle plumes do not move with respect to the geomagnetic (or spin) axis. Hence every volcano generated along a given hotspot track would record the magnetic inclination, usually expressed as the paleolatitude, of the site of present hotspot activity. If measured paleolatitudes are constant along the hotspot track, then the hotspot has not moved with respect to the spin axis. On the contrary, a change in hotspot paleolatitude with time would indicate motion of the mantle (because plumes are stationary within the mantle) relative to the spin axis, which is true polar wander. (Note that the low viscosity of the fluid outer core allows the geomagnetic field to remain coupled with the spin axis.)

*Hargraves and Duncan* [1973] first noted the systematic northward motion of hotspots in the Atlantic region and simultaneous southward motion of hotspots in the Pacific region, relative to the geomagnetic pole, over the past ~50 m.y. This observation was explained by a 12° clockwise rotation of the mantle about an equatorial axis emerging in the western Indian Ocean. Subsequent studies [*Morgan*, 1981; *Gordon and Cape*, 1981; *Harrison and Lindh*, 1982; *Livermore et al.*, 1983; *Andrews*, 1985; *Gordon and Livermore*, 1987; *Courtilot and Besse*, 1987] have confirmed this surprising conclusion and have determined a history of true polar wander since 200 Ma.



Figure 7 [from *Courtillot and Besse, 1987*] summarizes the latest comparison of plate motions measured in the two reference frames. In this illustration, apparent polar wander paths (paleomagnetic data) for all plates were transferred to the African apparent polar wander path by removing relative plate motions. This would be the apparent motion of the geomagnetic pole with respect to a (long-lived) observer on the African plate. The apparent motion of the hotspot reference frame with respect to Africa can also be described by a polar wander path. (In this case the rotation of the mantle relative to Africa, as inferred from the many hotspot tracks, is applied to the spin axis.) Gross features of the two paths are similar, but significant differences are seen by subtracting one curve from the other, to derive true polar wander.

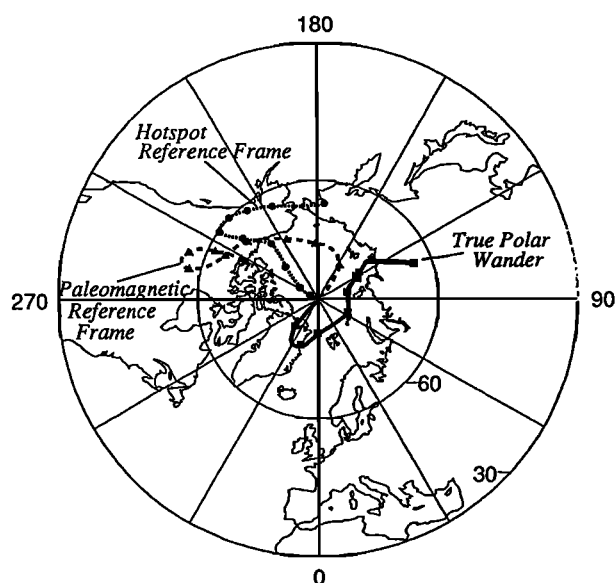


Figure 7. Comparison of the synthetic paleomagnetic apparent polar wander path (triangles, which are paleomagnetic pole positions for all plates rotated to the African plate, in present coordinates) with the synthetic path deduced from the hotspot reference frame (circles). True polar wander (squares) is calculated by subtracting one from the other; this represents global motion of the mantle with respect to the Earth's spin axis. Points on each curve are 20-m.y. increments, from 200 Ma to the present. Confidence intervals of 95% (not shown) are of the order of  $4^\circ$  [from *Courtillot and Besse, 1987*].

Approximately  $12^\circ$  of the true polar wander has occurred in the past 40 m.y., that is, clockwise rotation of the mantle about a pole on the equator, emerging near  $60^\circ\text{E}$  (western Indian Ocean). Between about 110 Ma and 40 Ma the mantle rolled nearly  $20^\circ$  about approximately the same pole but in the opposite direction, forming a hairpin turn in the true polar wander path at about 40 Ma (Figure 7). The period from 170 Ma to 110 Ma was remarkable because there was virtually no true polar wander; hotspots did not move with respect to the spin axis during this time. There is evidence for significant true

polar wander prior to Jurassic time, but its magnitude and direction are less certain because of the paucity of identifiable hotspot tracks older than 120 Ma.

Intriguingly, the dramatic change in direction of true polar wander at 40 Ma occurred within a period of global plate motion reorganization to significantly more east-west collisional plate boundaries [*Rona and Richardson, 1978*]. The abrupt change in direction of the Pacific plate, reflected in the Hawaiian-Emperor bend (43 Ma), and the "hard" collision of India and Africa/Arabia against Eurasia occurred at this time. *Courtillot and Besse* [1987] concluded that these changes in subduction zone location and activity perturbed the torque balance of the coupled upper mantle-lithosphere system, which then altered the direction of true polar wander. The earlier 60-m.y. period when no true polar wander occurred is correlated with a time of declining magnetic field reversal frequency and low lithospheric velocities which, *Courtillot and Besse* [1987] speculated, indicate a reduced state of mantle convection and decreasing instability in the outer core, probably linked by a lower heat flow across the core-mantle boundary.

#### 4. DO PLUMES SWAY IN THE MANTLE WIND?

Having surveyed the surface, volcanic expression of hotspots, let us now turn to the deeper convective regime of mantle plumes. The fixity of hotspots with respect to plate motions is difficult to explain with simple mantle convection models. In fact, no numerical or laboratory convection experiment has ever demonstrated such behavior, that is, plumes that are independent of upper boundary layer motions. Apparently, the source region for mantle plumes is decoupled from mantle flow associated with plate motions, presumably as a result of chemical and/or rheological stratification in the mantle. However, the lack of any self-consistent model is (and should be) troubling.

One approach to this problem is to consider the effect of horizontal shear in the upper mantle beneath a moving plate (the "mantle wind") upon a cylindrical plume rising through the mantle to form a hotspot. Shear flow bends the plume over horizontally, and some remarkable results have been obtained from laboratory fluid dynamical simulations of this flow interaction. Horizontally tilted plume conduits were first studied by *Skilbeck and Whitehead* [1978] and *Whitehead* [1982], who discovered that a tilted conduit of low-density material can break up into a series of individual rising blobs. This gravitational instability occurs for conduits deflected to greater than about  $60^\circ$  from the vertical (Figure 8). *Whitehead* [1982] suggested that this behavior may occur within a shallow shear zone beneath an oceanic plate, perhaps accounting for individual island volcanic centers along such hotspot tracks as the Hawaiian-Emperor chain (Figure 11a). *Olson and Singer* [1985] and *Olson and Nam* [1986] suggested

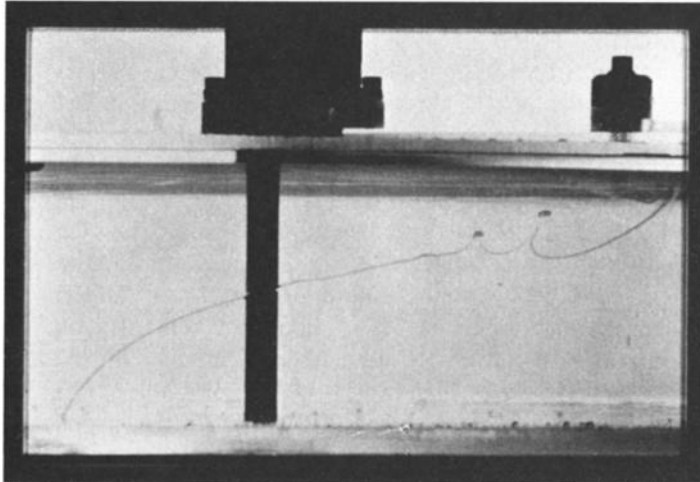


Figure 8. Photograph of a weak plume injected into a shear flow. The tilted conduit has developed a number of instabilities that are separating from the plume.

that a chain of rising blobs of mantle (diapirs) as large as 400 km in diameter may result from the same type of plume instability in the deep mantle. *Olson and Singer* [1985] also pointed out that the relative fixity of hotspots was not necessarily inconsistent with deflected, unstable plumes, at least for steady state mantle return flow.

In light of these phenomena it is natural to ask under what conditions plumes may or may not suffer significant horizontal deflection. Deflection of buoyant plume conduits by mantle shear flow beneath moving plates was studied in detail by *Richards and Griffiths* [1988]. Figures 9a–9c show a series of increasingly stronger mantle plumes deflected in a simple shear flow in laboratory experiments. In each of the photographs a cylindrical tank of glycerol is fitted with a lid which rotates and creates a shear flow in the tank. Motion is from left to right in the side-view photographs. A buoyant plume (80% glycerol and 20% water with red dye) is injected at a constant rate through a small hole in the bottom of the tank to the left of the dark vertical band formed by the rotational axis of the tank lid. The moving lid (“plate”) generates a cylindrical shear flow, with velocity increasing linearly from zero at the bottom of the tank. The plume trajectories are seen to be almost perfect parabolas, and *Richards and Griffiths* [1988] were able to model these trajectories accurately using a simple relation:

$$v = k\delta\rho g a^2 / \eta \quad (1)$$

where  $v$  is an effective Stokes rise velocity for a given plume conduit element,  $\delta\rho$  is the density contrast between the plume and surrounding fluid,  $g$  is the gravitational acceleration,  $a$  is the plume radius, and  $\eta$  is the viscosity of the surrounding fluid;  $k$  is a constant determined empirically from the experiments ( $k = 0.54 \pm 0.02$ ).

The above relation can be used to calculate a plume trajectory in a fluid layer, if the background flow in the layer (e.g., due to plate motion) is known. One simply calculates the trajectory of a Stokes conduit element released from the plume origin from a combination of its rise velocity  $v$  and advection due to motion in the surrounding fluid. The combination of the simple linear shear flow in the experimental tank and the constant Stokes rise velocity of the plume conduit results in the parabolic trajectories shown in Figure 9.

Although the experiments shown have a particularly simple flow geometry, it is possible to use (1) to model plume deflection under more realistic conditions. Figure 10 (top) illustrates again a simple shear flow, but with a large increase in viscosity at the level of the dashed line. The horizontal flow velocity is much larger in the low-viscosity region immediately beneath the plate, but the

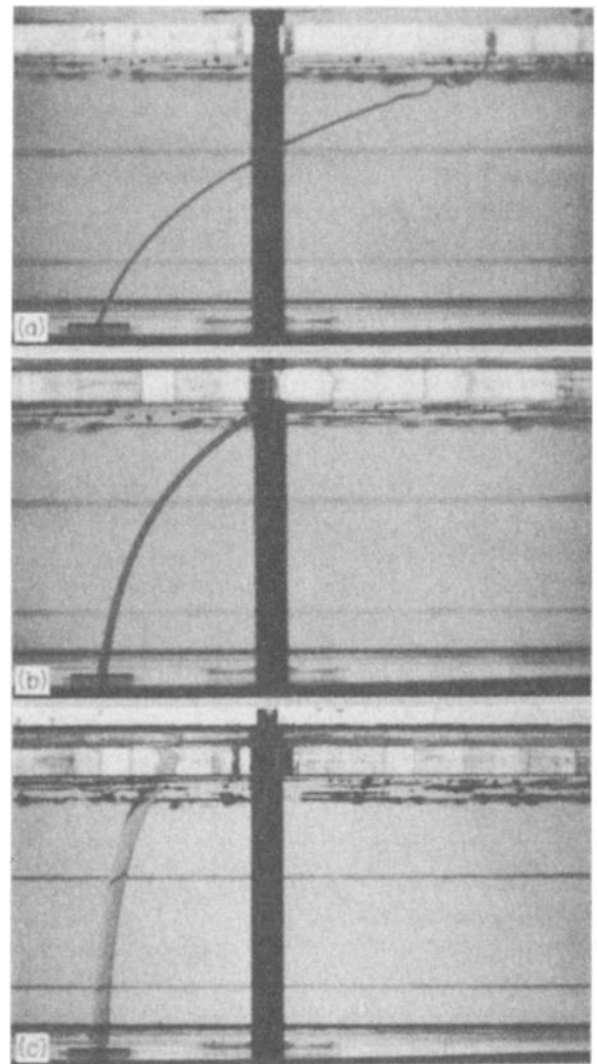


Figure 9. Photographs of laboratory tank experiments showing plume deflection by horizontal shear flow exerted by rotating surface plate [*Richards and Griffiths*, 1989].

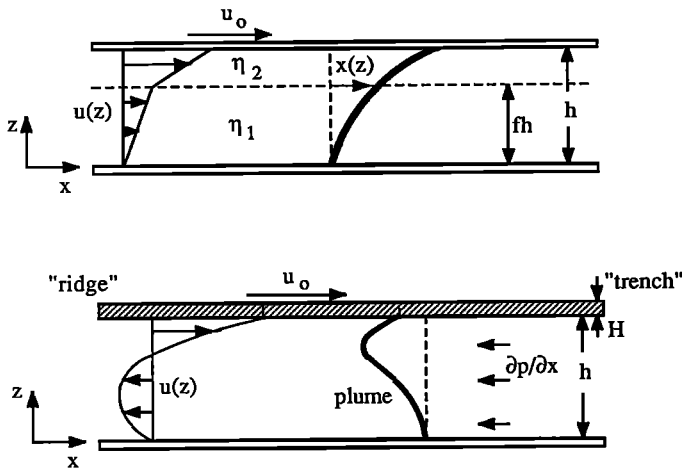


Figure 10. (Top) Diagram of plume deflection in a plate-driven shear flow with vertical viscosity stratification and (bottom) diagram of plume deflection in a simple return flow model.

steady state plume profile is unaffected. The higher horizontal flow velocity is just offset by the effect of the lower viscosity on the Stokes rise velocity of the plume conduit (see (1)). For steady state flow the low-viscosity zone does not prevent plume deflection. (However, it must be borne in mind that the part of the plume in the low-viscosity layer will adjust much more rapidly to changes in motion). In the example of Figure 10 (bottom) a return flow is added to account for trench-ridge mass balance in accord with the constant pressure model of *Turcotte and Schubert* [1982]. A more complicated plume trajectory results, with maximum horizontal deflection at about one fourth of the layer depth beneath the plate. (The bottom no-slip boundary condition in Figure 10 (bottom) is probably unrealistic. A free slip condition would result in a finite velocity at the bottom of the layer, with no vertical velocity gradient there.)

The Stokes velocity characterization, which was developed for steady state plume deflection, also accurately describes the transient adjustment of plumes to changes in the background shear flow [*Richards and Griffiths*, 1988]. This leads to a very specific application of (1) above, namely, the adjustment of the Hawaiian plume to the change in Pacific plate motion which occurred about 43 million years ago, resulting in the Hawaiian-Emperor bend (Figure 11a). Figure 11b shows a map view of the theoretical surface trace of a deflected mantle plume, subject to a 60° change in plate motion (comparable to the change in Pacific plate motion at 43 Ma). The "track" starts at the top left with steady plate motion (speed  $U$ ) at N30°W, and then adjusts to due westerly plate motion (also speed  $U$ ) with the newest "volcano" at the far right. In this model, there is simple shear flow beneath the plate in a fluid layer of depth  $h$ . The Stokes rise velocity of the plume conduit is  $v$ . The

N-S and E-W spatial scales in Figure 11b are normalized by the factor  $Uh/2v$ , which is the maximum horizontal deflection of the plume. With this normalization the approximate radius of curvature of the bend in the surface

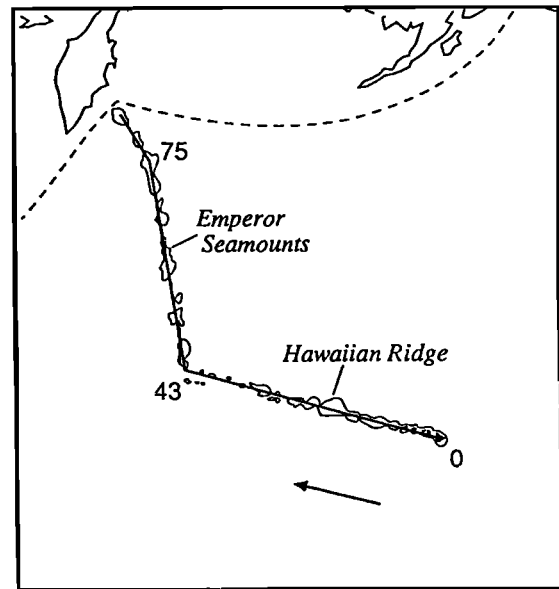


Figure 11a. The volcanic trail of the Hawaiian hotspot on the Pacific plate (present direction indicated by arrow). Ages along the lineament are in millions of years; an abrupt change in plate direction occurred at 43 Ma, and a lesser one occurred at 75 Ma.

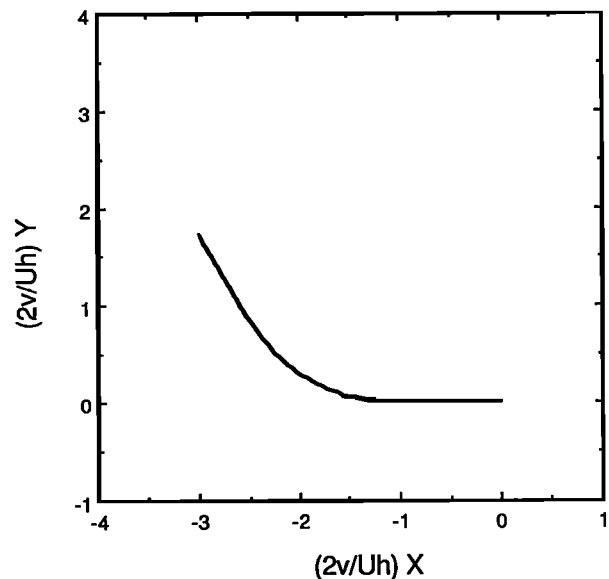


Figure 11b. A theoretical plume track relative to a moving plate which undergoes an instantaneous change in direction through 60° with no change in speed is also shown. The plume rises through a layer of constant shear. Spatial coordinates are nondimensionalized so that unit distance is the maximum horizontal deflection. This becomes the radius of curvature for the bend.

trace is seen to be about 1. In other words, Figure 11*b* shows the intuitive result that the radius of curvature of the plume trace in response to the change in plate motion is approximately equal to the maximum horizontal deflection of the plume. This theoretical result was shown to be quite accurate in laboratory experiments simulating a plate motion change [Griffiths and Richards, 1989].

The Hawaiian-Emperor bend itself has a radius of curvature of no more than about 100–200 km (Figure 11*a*). (See for example, Jackson *et al.* [1972] for detailed bathymetry.) Of course, some apparent curvature must result from the finite width of the trace itself and, perhaps, a noninstantaneous change in plate motion. From the above theoretical considerations it is clear that the observed sharpness of the Hawaiian-Emperor bend constitutes a first-order observation concerning the dynamics of the Hawaiian plume. The Hawaiian plume cannot be horizontally deflected more than about 200 km in the region of the upper mantle that is strongly coupled to plate motions. This was first pointed out by Whitehead [1982], who suggested that the Hawaiian plume might be strongly deflected within a shallow shear zone (~200 km deep) beneath the Pacific plate, giving rise to individual island volcanic centers via conduit instability. However, an additional condition for such an instability is that the plume diameter be much less than the layer depth; otherwise the diapirs would not have sufficient room in which to form. Alternatively, the plume may be vertical through the entire upper mantle, and the formation of individual volcanic centers might be controlled by lithospheric strength and heterogeneity.

Using (1), it is instructive to calculate the size of plume necessary to remain vertical in the face of the mantle wind beneath the Pacific plate. An appropriate criterion would be that the vertical Stokes rise velocity  $v$  associated with the Hawaii plume is not much less than the overriding plate velocity of about 100 mm/yr. Setting  $v_s \geq 10$  mm/yr and using reasonable values for upper mantle viscosity  $\eta = 10^{22}$  P and plume density contrast  $\delta\rho = 0.05$  g/cm<sup>3</sup>, this requires a plume diameter  $d = 2a > 70$  km. This is consistent with Morgan's [1972] original estimate for plume width based on the gravity anomaly over Hawaii and is certainly a reasonable value.

More remarkable perhaps than the spectacular Hawaiian-Emperor bend is the fact that much weaker hotspot tracks also appear to represent "absolute" plate motions quite reliably. Although there are no other similarly distinct bends, our ability to formulate a fixed hotspot reference frame shows that other hotspots in the Pacific, Atlantic, and Indian oceans are not undergoing significant transient adjustment to overlying plate motions. In addition to the well-known major hotspots mentioned in previous sections, several seamount chains which are tiny by comparison also appear to record plate motion faithfully. The Cobb-Eickelberg seamounts in the northeast Pacific have been shown by radiometric dating to be explainable by a fixed hotspot active since at least 10 Ma,

now located at the present-day Juan de Fuca spreading center [Desonie and Duncan, 1990]. In the Tasman Basin east of the Australian continental margin the Tasmantid Seamounts have been shown to represent Australia-Indian plate motion over three fixed hotspots since at least 24 Ma, forming three parallel seamount/volcano chains (Figure 6 [McDougall and Duncan, 1988]). Since these hotspots are at least an order of magnitude weaker than Hawaii (e.g., in terms of volcanic production rates or associated bathymetric swells), it is even more remarkable that these seamount chains are consistent with the hotspot reference frame.

Although it is plausible that plumes remain vertical beneath fast plates, we have not justified the fixity of the plume sources. Thermal plumes must originate from a thermal boundary layer, and either the core-mantle boundary (for mantle-wide convection) or a hypothetical boundary layer in the mantle transition zone (for chemically layered convection) is the only plausible source region. Motions at the core-mantle boundary may be effectively decoupled from plate-related convective flow by an increase in mantle viscosity with depth by about a factor of 100–1000 (see, for example, Gurnis and Davies [1986]). A boundary layer at 670 km depth presents a greater difficulty since trench-ridge return flow is confined to the upper mantle, regardless of the viscosity structure. Global models for deep mantle flow derived from plate motions [Hager and O'Connell, 1981] and from attempts to model seismically imaged mantle heterogeneity and the geoid [Forte and Peltier, 1987; Richards and Hager, 1988] yield midmantle velocities somewhat smaller than plate velocities but generally greater than about 5 mm/yr. Therefore it is not clear how a midmantle boundary layer source for hotspot plumes could provide an absolute reference frame with respect to plate motions [Richards, 1991].

## 5. ARE FLOOD BASALTS THE RESULT OF PLUME INITIATION?

The origin of continental flood basalt eruptions has remained a major geological mystery which has not been solved by any aspect of the theory of plate tectonics. Recently, much attention has been focused on the geological, geochemical, and geodynamical nature of these extraordinary events, and this interest results in large part from the clear association of flood basalt events with the beginning of hotspot tracks as well as the coincidence of the spectacular Deccan flood basalt eruptions with the Cretaceous-Tertiary mass extinction event [Duncan and Pyle, 1988; Courtillot *et al.*, 1988]. The association of flood basalts and hotspots [Morgan, 1972, 1981] is shown in Figure 12, and spatial and temporal relationships such as that between the Réunion hotspot and the Deccan eruptions are now firmly documented by precise K-Ar and <sup>40</sup>Ar–<sup>39</sup>Ar dating [Duncan and Hargraves, 1990]. These

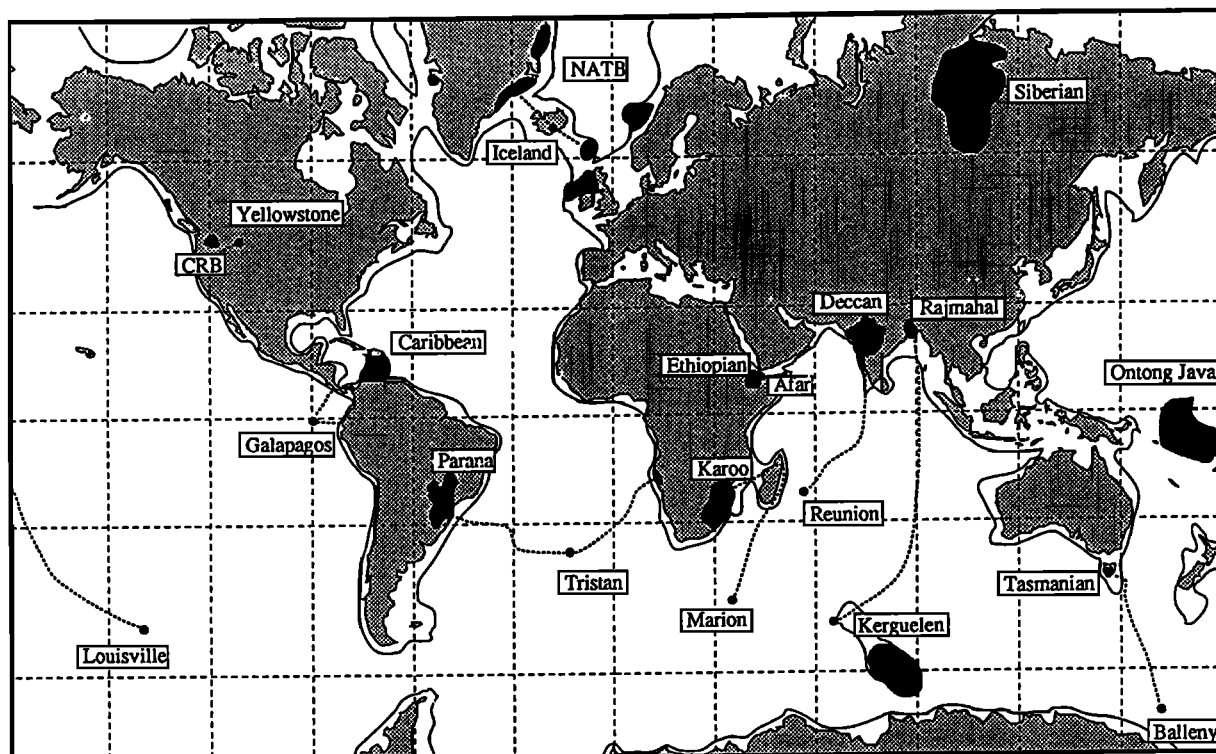


Figure 12. Worldwide distribution of flood basalt provinces erupted in the last 250 m.y. and associated hotspots (where known or conjectured). Note that while many occur along conti-

ental margins, others have formed in continental interiors or in ocean basins. CRB are Columbia River basalts, and NATB are North Atlantic Tertiary basalts.

hotspot/flood basalt correlations also include Iceland/North Atlantic Tertiary basalts, Tristan da Cunha/Parana-Etendeka basalts, Marion/Karoo basalts, Yellowstone/Columbia River basalts, and Kerguelen/Rajmahal traps. In addition, some major oceanic basalt plateaus (e.g., Ontong-Java, Caribbean) may mark the initial activity of hotspots (Louisville, Galapagos). Of all the major flood basalt provinces only the Siberian traps lack a clear association with a known hotspot track, perhaps because of our poor knowledge of the Arctic Ocean basin.

#### Passive Rifting or Plume Initiation?

Many of the continental flood basalt eruptions are associated with the early stages of continental breakup and rifting (North Atlantic, Parana, Karoo, Deccan), and this observation has given rise to a number of models for their origin based on rifting [e.g., Cox, 1980; Bott, 1982; White *et al.*, 1987; Meissner and Kopnick, 1988]. Morgan [1981] proposed two related hypotheses: (1) that continental lithosphere was weakened by the long-term activity of a hotspot, which warmed the upper mantle (asthenosphere) beneath the continent and led to massive eruptions derived from this material during extension and rifting; and (2) that the large "head" of a new mantle plume results first in a massive melting event, followed by more modest activity along the ensuing hotspot track because of the remaining steady plume. These two models are closely related and, upon superficial examination, may seem almost indistin-

guishable in terms of the geological record. However, their implications concerning the relationship between continental breakup and plumes, the origin of plumes themselves, and the processes of melting in flood basalt events are different in important ways. White and McKenzie [1989] have recently developed a detailed formulation of the more passive and uniformitarian rifting model, providing an elegant explanation for the presence of huge basalt accumulations along rifted continental margins but placing little emphasis on how plumes begin and reach the base of the lithosphere. Richards *et al.* [1989] have emphasized the merits of the plume initiation model in explaining the extraordinary eruption rates and sudden onset of flood basalt volcanism, also suggesting that rifting is not a necessary prerequisite to the initial stages of volcanism. Campbell *et al.* [1989] further suggested that Archean greenstone terranes (thick sequences of low-temperature altered basaltic rocks) may be the remnants of plume initiation events.

Both models require the presence of a broad reservoir of anomalously hot mantle beneath the lithosphere. The rifting model developed by White and McKenzie [1989] is very specific about how melt is generated. A plume (steady or otherwise) warms the sublithospheric mantle to temperatures as much as 200°C in excess of the normal mantle potential temperature of 1280°, which is typically found beneath mid-ocean spreading ridges far removed from hotspots. Large degrees of extension (factors of at

least 2–4) in the overlying continental lithosphere cause decompression melting of the hot plume material, producing a melt thickness of about 25 km (as compared with 7 km for normal melting at spreading ridges) that erupts to fill the rift. Thus a huge amount of melt is generated when a continent rifts above an active mantle plume, as opposed to normal mantle. This model has been applied to the development of the volcanic rift margins of the North Atlantic Tertiary Province (Figures 4 and 12 [White *et al.*, 1987]) and is most successful in explaining the great thicknesses of onlapping basalt (and perhaps underlying intrusive) structures mapped in seismic reflection profiles of the Hatton Bank and Vøring Plateau margins on the eastern margins of the North Atlantic [Eldholm *et al.*, 1989]. Cox [1989] has also invoked this model for the evolution of volcanic continental margins to explain the development of drainage systems following the Deccan, Parana, and Karoo flood basalt events. Despite the objections we raise below, the White and McKenzie model provides a useful quantitative framework for understanding the evolution of volcanic continental margins subsequent to rifting (for example, see Cox [1989]).

The plume initiation hypothesis was originally based upon the largely circumstantial evidence (1) that flood basalts often represent the earliest activity of hotspots and (2) that the truly catastrophic nature of flood basalt events required some special cause other than one associated with the time scale for plate motions. The first of these observations is questionable, since it is possible that such hotspots as Réunion and Tristan da Cunha cannot normally penetrate stable continental lithosphere. The second observation is more compelling because the alternative rifting mechanism described above predicts the duration of flood basalt events to be of the order of ~10 m.y., clearly in disagreement with evidence for ~1 m.y. (or smaller) time scales for some events such as the Deccan basalts [Duncan and Pyle, 1988; Courtillot *et al.*, 1988; Baksi and Kunk, 1988]. Also, as we describe in some detail below, laboratory and numerical models suggest that plume initiation may be expected to result in a huge volcanic event at the beginning of a hotspot track.

Although this evidence is suggestive, we find that the observed tectonic settings for flood basalt events provide compelling evidence that these eruptions do not, in general, result from decompression melting in response to lithospheric extension. In fact, many flood basalt events are neither preceded nor accompanied by large degrees of extension. Many examples may be cited: (1) The main tholeiitic eruptions of the Deccan Traps preceded significant extension along the west coast of India [Hooper, 1990], while much smaller (volumetrically) eruptions of more alkalic lavas (typical of volcanism associated with extension in other areas) accompanied the extension and rifting event which carried the Seychelles Bank westward. Furthermore, the Indian subcontinent was moving very rapidly over the mantle (~150–180 mm/yr) at the time of the Deccan eruptions, thus precluding any large accumula-

tion of hot plume material beneath the plate due to “ordinary” Réunion plume activity. (2) The main sequence of tholeiitic basalt lavas in the Parana event in South America preceded significant extension in that area [Piccirillo *et al.*, 1988a, b], again with smaller, more alkalic basalt eruptions accompanying the extension that eventually led to continental breakup. (3) The large ~195-Ma central area tholeiitic basalt eruptions of the Karoo province (Lesotho) are associated with geochemically identical feeder dike complexes which are pervasive throughout a very broad area of what is clearly unrifted, stable continental lithosphere [Marsh, 1987]. “Associated” rifting about 20 m.y. later between Africa and Antarctica was accompanied by huge alkalic basalt eruptions that shifted toward the rifting margin. (4) The Grande Ronde eruptions of the Columbia River Basalt Group were accompanied by at most ~1% crustal extension [Hooper, 1990], with subsequent extension (~20%) associated with more silica-rich eruptions. (5) The Siberian Traps were preceded by a long “geosynclinal” period, but structures disrupted by these huge intracontinental eruptions show no evidence of significant extension either prior to or during flood volcanism [Makarenko, 1976]. Hence the Siberian Traps volcanism did not coincide with major continental rifting. (6) Even in the North Atlantic Tertiary Province, where the rifting model has found detailed application, it is not obvious that all of the flood basalt eruptions were accompanied by large degrees of extension. For example, the famous dike complex of Skye (western Scotland), which fed some of the tholeiitic flood basalt eruptions, indicates only mild extension oriented perpendicular rather than parallel to the direction of subsequent rifting.

From this evidence we conclude that most flood basalt events result from melting events at the base of the lithosphere, whether or not such thermal events precipitate subsequent rifting. Therefore we must appeal to an extraordinary pulse of mantle plume material far in excess of the flux represented by the subsequent hotspot track. This gives rise to an interesting and fundamental question: Can large degrees of partial melting (say 10–20%) occur at the base of normal continental lithosphere in the absence of significant mechanical thinning (rifting)? Although we will not attempt a full discussion, a partial answer to this question is found by referring to recent mantle melting models based upon melting experiments on candidate mantle rocks and upon observations of major and trace element variations in ocean ridge basalts and peridotites (Mg, Fe silicate rocks thought to be representative of upper mantle material). Both McKenzie and Bickle [1988] and Klein and Langmuir [1987] conclude that excess temperatures of about 250°C above ambient are required to obtain large melt fractions at depths of about 70–100 km. Although this value is somewhat larger than some estimates of maximum hotspot temperatures [Courtney and White, 1986], it is at least consistent with those suggested by others [Jacques and Green, 1980]. Hence the difference with regard to melt production between the plume



initiation model and the rifting model for melt production is that we assume a slightly higher temperature for at least the leading diapir of a starting mantle plume [Richards *et al.*, 1989] than that advocated by White and McKenzie [1989]. (It should also be noted that these inferred temperatures result from experiments on water-free melts and that the presence of volatiles, particularly CO<sub>2</sub>, in the more enriched plume source material may enhance the degree of melting at depth or produce melting at lower temperatures [Wyllie, 1977].

We emphasize that neither the tectonic nor the petrological constraints on the nature of flood basalt eruptions are conclusive. More field work needs to be directed toward elucidating the field relations we have attempted to summarize, and this aspect of the problem has been neglected in comparison to the enormous amount of work on the petrology and geochemistry of flood basalts exemplified by several recently published reviews [Macdougall, 1988]. We have made no attempt to summarize this vast literature here, and the main purpose of our brief review is to emphasize the importance of field observations concerning the relations between crustal extension and flood basalt volcanism.

In addition to models based on mantle plume activity, Rampino and Stothers [1988] have suggested that flood basalt eruptions are triggered by meteorite impact. This remarkable hypothesis results mainly from the association of some flood basalt events with extinction events, in particular, the Deccan basalts with the Cretaceous-Tertiary (K-T) boundary events and, possibly, the Siberian basalts with the Permo-Triassic extinctions. This impact origin for flood basalts is inferred largely from the coincidence of the Deccan volcanism with the K-T boundary, but a generalized model for flood basalt volcanism and associated post impact hotspot track activity has not been formulated. In our opinion the impact hypothesis for flood basalt and hotspot volcanism lacks physical plausibility (and craters). However, the apparent coincidence of two of the largest flood basalt events (Deccan, Siberian) with the two largest extinction events further suggests the potential importance of developing a detailed understanding of the dynamical origins of flood basalt volcanism. In the remaining discussion we briefly discuss the fluid dynamics of the plume initiation model. Having stated our preference for the plume initiation model [Richards *et al.*, 1989], the following discussion reflects our bias against the passive rifting model.

### Starting Plumes

Given that mantle plumes have for some time been widely accepted as the likely cause of hotspot tracks, it seems strange that little work has been directed at the question, How do plumes start? The answer appears to be "Spectacularly!" at least in the cases involving flood basalt eruptions. Simple laboratory experiments [Whitehead and Luther, 1975] show that this behavior is to be expected from starting plumes, especially if the plumes have

significantly lower viscosity than the material through which they rise. Figure 13a shows such a plume formed by steady injection of dyed water into higher-viscosity and higher-density glucose syrup. A very large "head" forms at the top of the plume, followed by a thin, connected conduit ("tail") of buoyant fluid. Hence the possible analogy to flood basalts and hotspot tracks as plume heads and tails is noted [Richards *et al.*, 1989; Campbell *et al.*, 1989].

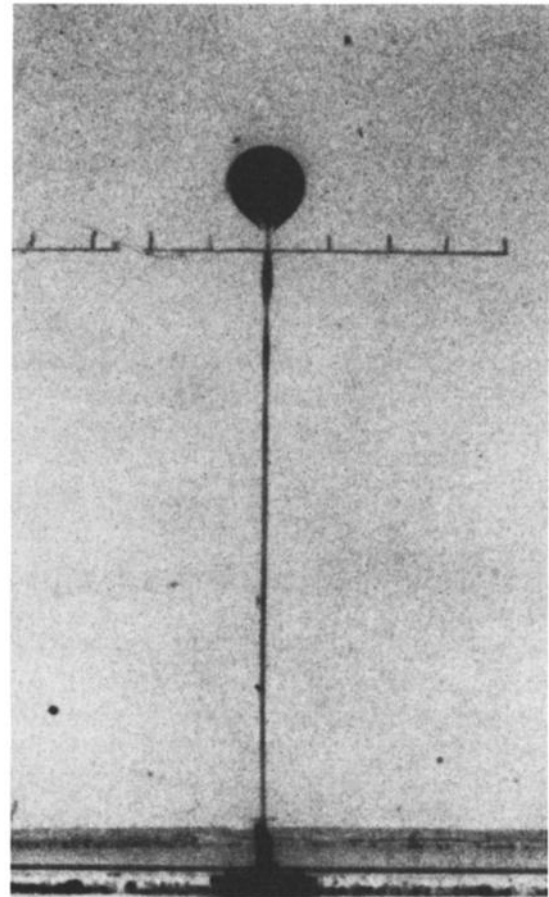


Figure 13a. Photograph of a plume head followed by a trailing conduit. The plume is formed by injection of water (colored with red dye) at a constant rate into the bottom of a large tank of glucose.

The stark contrast between plume head size and feeder conduit width is mainly a result of the viscosity contrast between the plume and the surrounding material. The larger the viscosity contrast, the thinner the conduit. This can be understood easily. The rise of the plume through the fluid is governed almost entirely by the "Stokesian" rise of the plume head through the surrounding material [Olson and Singer, 1985], while the conduit must supply the growing plume according to the volumetric feed rate (an artifice addressed below). The lower the plume viscosity, the narrower the plume conduit [Whitehead and Luther, 1975]. Returning to the hotspot analogy, this relationship may explain the very narrow apparent width of

mantle plumes (~10–100 km) compared to the large areal extent of flood basalt events. Of course, a large viscosity contrast between the plume and the surrounding mantle is expected if the plume buoyancy is derived from temperatures exceeding the surrounding mantle by perhaps several hundred degrees Celsius [McKenzie and Bickle, 1988; Sleep, 1990].

On the basis of this simple model of diapiric instability and rise we have shown, for reasonable choices of mantle viscosity ( $10^{22}$  P) and plume density contrast ( $0.1 \text{ g/cm}^3$ ), that a starting plume fed by a conduit sufficient to account for volcanism along the Réunion hotspot track will achieve a minimum volume of about  $5 \times 10^6 \text{ km}^3$  [Richards *et al.*, 1989] (see Griffiths and Campbell [1990] for a more detailed discussion of this type of estimate). Extensive melting of such a plume head beneath the lithosphere would account for the large volume of lavas in the Deccan eruptions ( $1\text{--}2 \times 10^6 \text{ km}^3$ ). In this context it is important to note that the resulting magma would have a high olivine content [Campbell and Griffiths, 1990] and that basaltic magmas would result from olivine crystallization and removal at a density trap somewhere above the crust-mantle boundary (Moho) at a typical depth of 30–40 km. Such a fractionation process is well documented for the tholeiites of the Columbia River basalts [Hooper, 1988], and the plume initiation model suggests, at least in the cases where huge eruptions precede large-scale extension, that flood basalts may not represent primary magmas.

One interesting aspect of thermal plumes is the process of entrainment of surrounding mantle during their ascent [Griffiths, 1986; Richards and Griffiths, 1989]. Such mixing has important consequences for the geochemical signatures of both hotspot and flood basalts, and it is of particular interest in light of the often enriched trace element contents and isotope ratios associated with these lavas [Zindler and Hart, 1986]. In plumes driven by compositional buoyancy as in Figure 13a, there is little mixing between the two fluids. However, in plumes driven by thermal buoyancy, thermal diffusion causes surrounding material to become buoyant and rise along with the plume. This is shown in Figure 13b [from Griffiths and Campbell, 1990], where a hot, dyed starting plume of glucose wraps laminae of clear surrounding glucose into the head as it rises. If the original plume material is fertile lower mantle, then the compositionally distinct (depleted in certain elements by repeated melting episodes) upper mantle material will be entrained into the plume head, resulting in a complicated mixing process as melting and volcanic eruptions occur. A particularly interesting aspect of Griffiths and Campbell's analysis is the manner in which the mantle acts as a plume buoyancy flux filter in thermally dissipating weak plumes (i.e., plume instabilities with effectively low Rayleigh numbers). They concluded that the strongest starting plumes maintain temperature excesses of  $\sim 250^\circ\text{C}$  in rising through the mantle (with only a small fraction of entrained material), while the weakest plumes that make it to the

surface must be about  $50^\circ\text{C}$  hotter (with only a small fraction of original plume source material).

The experiments shown in Figure 13 are artificial in the sense that the plumes are injected (at a constant rate) and are not the result of the type of thermal convective instability likely to occur at an internal boundary layer such as the core-mantle boundary. Unfortunately, no laboratory or numerical convection experiments have been conducted in the regime thought appropriate to the formation of mantle plumes. Such starting plumes are expected to arise in time-dependent, three-dimensional, thermal convection at very high Rayleigh number in fluids with strongly temperature-dependent viscosity, but these conditions have not yet been reached in simulations. Therefore this represents a gap in our ability to model starting plumes satisfactorily and to understand fully how to relate observation and theory, especially in regard to hotspots and flood basalts.

Perhaps the experiments that come closest to exhibiting the expected starting behavior are those of Olson *et al.* [1988] in which two-dimensional plumes were generated in a pulse heating mode. Plume development in one such numerical experiment is shown in Figure 14 [from Olson *et al.*, 1988, Figure 18], where a layer cooled initially from



Figure 13b. Photograph of a starting thermal plume formed by injection of hot, dyed glucose into a tank of cooler, clear glucose [from Griffiths and Campbell, 1990].



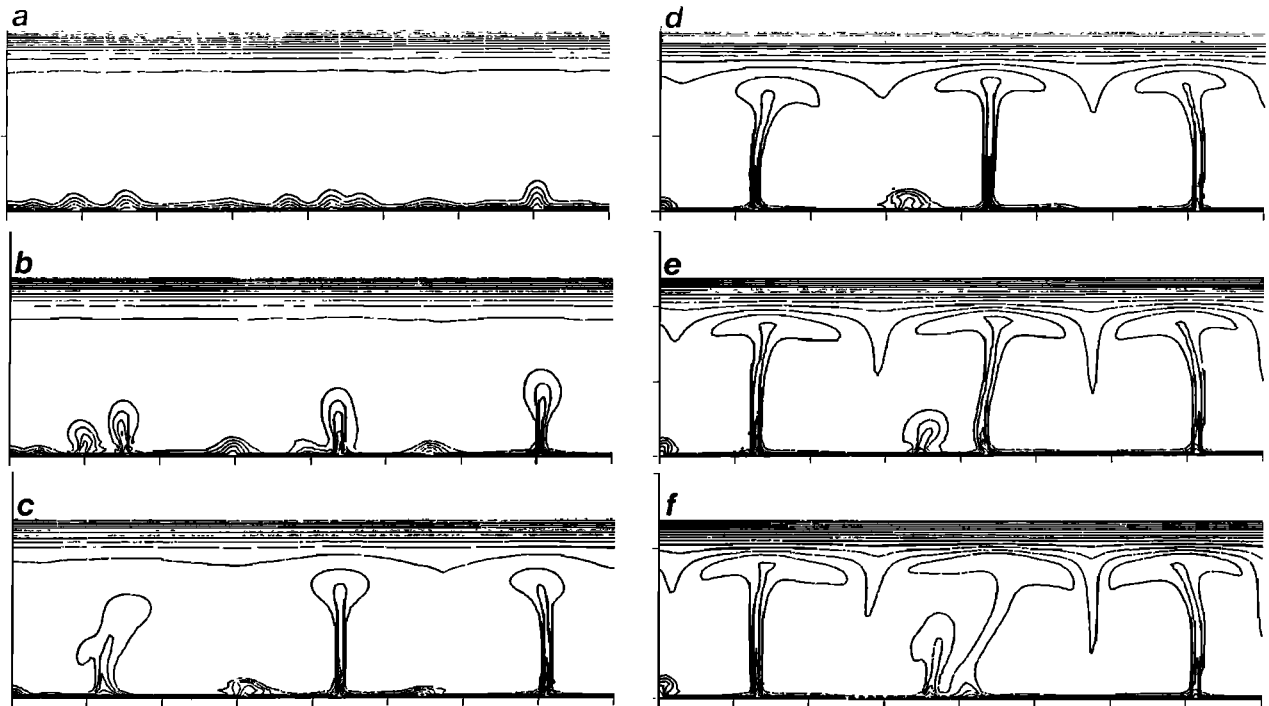


Figure 14. Isotherms from numerical pulse-heating experiments on plume-lithosphere interaction with temperature-dependent

rheology at approximately 10-m.y. intervals [from *Olson et al.*, 1988].

above (yielding a stiff lithosphere) is suddenly heated uniformly from below. The fluid has a mildly temperature-dependent viscosity, with maximum contrast of a factor of 1000. Plume instabilities form and coalesce, then rise to the top, followed by narrower, connected plume "conduits." This study shows that the trailing plume conduits become thinner compared with the starting plumes as the viscosity contrast is increased, as expected on the basis of the simpler injection experiments. However, we emphasize that even these experiments are inadequate and artificial. The Earth, in three dimensions, is likely to exhibit stronger contrasts in rheological behavior and probably does not conduct pulse-heating experiments. (This is not a criticism of *Olson et al.*'s experiments, since they were directed toward understanding plume-lithosphere interaction more than plume formation.) Clearly, there is a need for better convection experiments in order to understand even this very basic phenomenon of plume initiation.

There is no doubt that some flood basalt events are related to continental rifting, but the cause and effect relationship between volcanism and rifting is unclear. Because not all continental rift margins show a phase of flood volcanism, even a model in which rifting plays a major role in melt generation must involve extraordinary circumstances. A crucial distinction between the passive rift and the active plume initiation models will be whether certain oceanic plateaus, such as the Ontong-Java plateau

(Figure 12), are flood basalt provinces, equivalent to the continental examples. We expect that basalt ages across the entire Ontong-Java plateau are contemporaneous. Recently completed deep sea drilling (Ocean Drilling Project leg 130) has recovered thick, flood-type basalt flows that are contemporaneous with submarine-erupted flow sequences exposed at the islands of Malaita and Santa Isabel, at the southern margin of the plateau [*Kroenke et al.*, 1990].

## 6. CONCLUSIONS

More than a peculiar volcanic phenomenon that has defied plate tectonic classification, hotspot volcanism appears to be a manifestation of whole-mantle convection via plume flow. While we have focused on the kinematics and dynamics of hotspots and plumes, the geochemical characteristics of hotspot provinces indicate that plumes deliver material from the lower mantle that is primordial or has been accumulating over billions of years of plate subduction [e.g., *Zindler and Hart*, 1986]. The pattern of hotspots is stable within useful time scales because plumes originate in the deep mantle where the viscosity structure permits only horizontal velocities that are much lower than plate velocities; plumes are not significantly deflected by upper mantle horizontal flow. Plume initiation is governed by heat flowing from the core to the lower mantle. Diapir

formation and rise result in vast amounts of melting from the plume head. This flood basalt phase is followed by an age-progressive hotspot track that is supplied by melting of the plume tail. Further studies of continental and oceanic flood basalt provinces should better constrain the time scale, fluid dynamics, and heat flux of these important events. It is clear that hotspot traces form a rich source of constraints on the dynamical, compositional, and thermal histories of the deep mantle which we have hardly begun to utilize.

**ACKNOWLEDGMENTS.** This research was supported by the National Science Foundation and the Office of Naval Research.

David Scholl was the editor responsible for this paper. He thanks David Engebretson and Richard Carlson for their assistance in evaluating the technical content and Eric Wood for serving as a cross-disciplinary referee.

## REFERENCES

- Andrews, J. E., True polar wander: An analysis of Cenozoic and Mesozoic paleomagnetic poles, *J. Geophys. Res.*, **90**, 7737–7750, 1985.
- Baksi, A. K., and M. J. Kunk, The age of initial volcanism in the Deccan Traps, India: Preliminary  $^{40}\text{Ar}/^{39}\text{Ar}$  age spectrum dating studies, *Eos Trans. AGU*, **69**, 732, 1988.
- Bott, M. H. P., The mechanism of continental splitting, *Tectonophysics*, **81**, 301–309, 1982.
- Burke, K., W. S. F. Kidd, and J. T. Wilson, Relative and latitudinal motion of Atlantic hot spots, *Nature*, **245**, 133–137, 1973.
- Campbell, I. H., and R. W. Griffiths, Implications of mantle plume structure for the evolution of flood basalts, *Earth Planet. Sci. Lett.*, **99**, 79–93, 1990.
- Campbell, I. H., R. W. Griffiths, and R. I. Hill, Melting in an Archaean mantle plume: Heads its basalts, tails its komatiites, *Nature*, **339**, 697–699, 1989.
- Cande, S., J. L. LaBrecque, and W. B. Haxby, Plate kinematics of the South Atlantic: Chron 34 to present, *J. Geophys. Res.*, **93**, 13,479–13,492, 1988.
- Clague, D. A., and R. D. Jarrard, Tertiary Pacific plate motion deduced from the Hawaiian-Emperor chain, *Geol. Soc. Am. Bull.*, **84**, 1135–1154, 1973.
- Courtilot, V., and J. Besse, Magnetic field reversals, polar wander, and core-mantle coupling, *Science*, **237**, 1140–1147, 1987.
- Courtilot, V., G. Feraud, H. Maluski, D. Vandamme, M. G. Moreau, and J. Besse, Deccan flood basalts and the Cretaceous/Tertiary boundary, *Nature*, **333**, 843–846, 1988.
- Courtney, R. C., and R. S. White, Anomalous heat flow and geoid across the Cape Verde Rise: Evidence for dynamic support from a thermal plume in the mantle, *Geophys. J. R. Astron. Soc.*, **87**, 815–867, 1986.
- Cox, K. G., A model for flood basalt volcanism, *J. Petrol.*, **21**, 629–650, 1980.
- Cox, K. G., The role of mantle plumes in the development of continental drainage patterns, *Nature*, **342**, 873–877, 1989.
- Crough, S. T., Mesozoic hotspot epeirogeny in eastern North America, *Geology*, **9**, 2–6, 1981.
- Crough, S. T., and D. M. Jurdy, Subducted lithosphere, hot spots, and the geoid, *Earth Planet. Sci. Lett.*, **48**, 15–22, 1980.
- DeMets, C., R. G. Gordon, and D. Argus, Intraplate deformation and closure of the Australian-Antarctic-Africa plate circuit, *J. Geophys. Res.*, **93**, 11,877–11,897, 1988.
- Desonie, D. L., and R. A. Duncan, The Cobb-Eickleberg seamount chain: Hotspot volcanism with MORB affinity, *J. Geophys. Res.*, **95**, 12,697–12,711, 1990.
- Duncan, R. A., Geochronology of basalts from the Ninetyeast Ridge and continental dispersion in the eastern Indian Ocean, *J. Volcanol. Geotherm. Res.*, **4**, 283–305, 1978.
- Duncan, R. A., Hotspots in the southern oceans—An absolute frame of reference for motion of the Gondwana continents, *Tectonophysics*, **74**, 29–42, 1981.
- Duncan, R. A., Age progressive volcanism in the New England seamounts and the opening of the central Atlantic Ocean, *J. Geophys. Res.*, **89**, 9980–9990, 1984.
- Duncan, R. A., The age distribution of volcanism along aseismic ridges in the eastern Indian Ocean, *Proc. Ocean Drill. Program Sci. Results*, **121**, in press, 1991.
- Duncan, R. A., and D. A. Clague, Pacific plate motion recorded by linear volcanic chains, *The Ocean Basins and Margins*, vol. 7A, edited by A. E. M. Nairn, F. G. Stehli, and S. Uyeda, pp. 89–121, Plenum, New York, 1985.
- Duncan, R. A., and R. B. Hargraves, Plate tectonic evolution of the Caribbean region in the mantle reference frame, *The Caribbean–South American Plate Boundary and Regional Tectonics*, edited by W. E. Bonini, R. B. Hargraves and R. Shagan, *Mem. Geol. Soc. Am.*, **162**, 81–93, 1984.
- Duncan, R. A., and R. B. Hargraves,  $^{40}\text{Ar}$ – $^{39}\text{Ar}$  geochronology of basement rocks from the Mascarene Plateau, Chagos Bank and the Maldive Ridge, *Proc. Ocean Drill. Program Sci. Results, Leg 115*, 43–51, 1990.
- Duncan, R. A., and I. McDougall, Linear volcanism in French Polynesia, *J. Volcanol. Geotherm. Res.*, **1**, 197–227, 1976.
- Duncan, R. A., and D. G. Pyle, Rapid eruption of the Deccan flood basalts at the Cretaceous/Tertiary boundary, *Nature*, **333**, 841–843, 1988.
- Eldholm, O., J. Thiede, and E. Taylor, Evolution of the Vøring volcanic margin, *Proc. Ocean Drill. Program, Sci. Results, Leg 104*, 1033–1065, 1989.
- Engebretson, D. C., A. Cox, and G. Thompson, Correlation of plate motions with continental tectonics: Laramide to Basin-Range, *Tectonics*, **3**, 115–119, 1984.
- Engebretson, D. C., A. Cox, and R. G. Gordon, Relative motions between oceanic and continental plates in the Pacific basin, *Spec. Pap. Geol. Soc. Am.*, **206**, 56 pp., 1986.
- Forte, A. M., and W. R. Peltier, Plate tectonics and aspherical Earth structure: The importance of poloidal-toroidal coupling, *J. Geophys. Res.*, **92**, 3645–3679, 1987.
- Goldreich, P., and A. Toomre, Some remarks on polar wandering, *J. Geophys. Res.*, **74**, 2555–2567, 1969.
- Gordon, R. G., and C. D. Cape, Cenozoic latitudinal shift of the Hawaiian hotspot and its implications for true polar wander, *Earth Planet. Sci. Lett.*, **55**, 37–47, 1981.
- Gordon, R. G., and A. Cox, Paleomagnetic test of the early Tertiary plate circuit between the Pacific Basin plates and the Indian plate, *J. Geophys. Res.*, **85**, 6534–6546, 1980.
- Gordon, R. G., and R. A. Livermore, Apparent polar wander of the mean-lithosphere reference frame, *Geophys. J. R. Astron. Soc.*, **91**, 1049–1057, 1987.
- Griffiths, R. W., Thermals in extremely viscous fluids, including the effects of temperature-dependent viscosity, *J. Fluid Mech.*, **166**, 115–138, 1986.
- Griffiths, R. W., and I. H. Campbell, Stirring and structure in mantle plumes, *Earth Planet. Sci. Lett.*, **99**, 66–78, 1990.
- Griffiths, R. W., and M. A. Richards, The adjustment of mantle plumes to changes in plate motion, *Geophys. Res. Lett.*, **16**, 437–440, 1989.
- Gurnis, M., and G. F. Davies, Numerical study of high Rayleigh number convection in a medium with depth-dependent viscosity, *Geophys. J. R. Astron. Soc.*, **85**, 523–541, 1986.
- Hager, B. H., and R. J. O'Connell, A simple global model of plate dynamics and mantle convection, *J. Geophys. Res.*, **86**, 4843–4867, 1981.
- Hargraves, R. B., and R. A. Duncan, Does the mantle roll?, *Nature*, **245**, 361–363, 1973.

- Harrison, C. G. A., and T. Lindh, Comparison between the hotspot and geomagnetic field reference frames, *Nature*, 300, 251–252, 1982.
- Hartnady, C. J. H., and A. P. le Roex, Southern ocean hotspot tracks and the Cenozoic absolute motion of the African, Antarctic and South American plates, *Earth Planet. Sci. Lett.*, 75, 245–257, 1985.
- Hooper, P. R., The Columbia River Basalt, *Continental Flood Basalts*, edited by J. D. Macdougall, pp. 1–34, Kluwer Academic, Dordrecht, Netherlands, 1988.
- Hooper, P. R., The timing of crustal extension and the eruption of continental flood basalts, *Nature*, 345, 246–249, 1990.
- Irving, E., *Paleomagnetism and Its Application to Geological and Geophysical Problems*, John Wiley, New York, 1964.
- Jackson, E. D., E. A. Silver, and G. B. Dalrymple, Hawaiian–Emperor Chain and its relation to Cenozoic circum-pacific tectonics, *Geol. Soc. Am. Bull.*, 83, 601–618, 1972.
- Jaques, A. L., and D. H. Green, Anhydrous melting of peridotite at 0–15 kb pressure and the genesis of tholeiitic basalts, *Contrib. Mineral. Petrol.*, 73, 287–310, 1980.
- Jarrard, R. D., and D. A. Clague, Implications of Pacific island and seamount ages for the origin of volcanic chains, *Rev. Geophys.*, 15, 57–76, 1977.
- Jurdy, D. M., Relative plate motions and the formation of marginal basins, *J. Geophys. Res.*, 84, 6796–6802, 1979.
- Jurdy, D. M., The subduction of the Farallon plate beneath North America as derived from relative plate motions, *Tectonics*, 3, 107–113, 1984.
- Klein, E. M., and C. H. Langmuir, Global correlations of ocean ridge basalt chemistry with axial depth and crustal thickness, *J. Geophys. Res.*, 92, 8089–8115, 1987.
- Klitgord, K. D., and H. Schouten, Plate kinematics of the central Atlantic, *The Geology of North America, The Western North Atlantic Region, DNAG Ser.*, vol. M, edited by B. E. Tucholke and P. R. Vogt, pp. 351–378, Geological Society of America, Boulder, Colo., 1985.
- Kroenke, L., et al., *Proceedings of the Ocean Drilling Project Initial Reports, 130*, College Station, Tex., in press, 1990.
- Livermore, R. A., F. J. Vine, and A. G. Smith, Plate motions and the geomagnetic field, I, Quaternary and later Tertiary, *Geophys. J. R. Astron. Soc.*, 73, 153–171, 1983.
- Lonsdale, P., Geography and history of the Louisville hotspot chain in the southwest Pacific, *J. Geophys. Res.*, 93, 3078–3104, 1988.
- Macdougall, J. D., *Continental Flood Basalts*, 341 pp., Kluwer Academic, Dordrecht, Netherlands, 1988.
- Makarenko, G. F., The epoch of Triassic trap magmatism in Siberia, *Int. Geol. Rev.*, 19, 1089–1099, 1976.
- Marsh, J., Basalt geochemistry and tectonic discrimination within continental flood basalt provinces, *J. Volcanol. Geotherm. Res.*, 32, 35–49, 1987.
- Martin, A. K., Microplates in Antarctica, *Nature*, 319, 100–101, 1986.
- McDougall, I., and R. A. Duncan, Linear island chains—Recording plate motions?, *Tectonophysics*, 63, 275–295, 1980.
- McDougall, I., and R. A. Duncan, Age progressive volcanism in the Tasmanid seamounts, *Earth Planet. Sci. Lett.*, 89, 207–220, 1988.
- McKenzie, D. P., and M. J. Bickle, The volume and composition of melt generated by extension of the lithosphere, *J. Petrol.*, 29, 625–679, 1988.
- Meissner, R., and M. Kopnick, Structure and evolution of passive margins: The plume model again, *J. Geodyn.*, 9, 1–13, 1988.
- Minster, J. B., and T. H. Jordan, Present-day plate motions, *J. Geophys. Res.*, 83, 5331–5354, 1978.
- Minster, J. B., T. H. Jordan, P. Molnar, and E. Haines, Numerical modeling of instantaneous plate motions, *Geophys. J. R. Astron. Soc.*, 36, 541–576, 1974.
- Mitchell, C., G. K. Taylor, K. G. Cox, and J. Shaw, Are the Falkland Islands a rotated microplate? *Nature*, 319, 131–134, 1986.
- Molnar, P., and T. Atwater, Relative motions of hotspots in the mantle, *Nature*, 246, 288–291, 1973.
- Molnar, P., and J. Francheteau, The relative motion of hotspots in the Atlantic and Indian oceans during the Cenozoic, *Geophys. J. R. Astron. Soc.*, 43, 763–774, 1975.
- Molnar, P., and J. M. Stock, A method for bounding uncertainties in combined plate reconstructions, *J. Geophys. Res.*, 90, 12,537–12,544, 1985.
- Molnar, P., and J. Stock, Relative motions of hotspots in the Pacific, Atlantic and Indian oceans since Late Cretaceous time, *Nature*, 327, 587–591, 1987.
- Molnar, P., T. Atwater, J. Mammerickx, and S. M. Smith, Magnetic anomalies, bathymetry and the tectonic evolution of the South Pacific since the Late Cretaceous, *Geophys. J. R. Astron. Soc.*, 40, 383–420, 1975.
- Molnar, P., F. Pardo-Casas, and J. Stock, The Cenozoic and Late Cretaceous evolution of the Indian Ocean Basin: Uncertainties in the reconstructed positions of the Indian, African and Antarctic plates, *Basin Res.*, 1, 23–40, 1987.
- Morelli, A., and A. M. Dziewonski, Topography of the core-mantle boundary and lateral homogeneity of the liquid core, *Nature*, 325, 678–683, 1987.
- Morgan, W. J., Convection plumes in the lower mantle, *Nature*, 230, 42–43, 1971.
- Morgan, W. J., Deep mantle convection plumes and plate motions, *Am. Assoc. Pet. Geol. Bull.*, 56, 203–213, 1972.
- Morgan, W. J., Hotspot tracks and the opening of the Atlantic and Indian oceans, in *The Sea*, vol. 7, edited by C. Emiliani, pp. 443–475, Wiley Interscience, New York, 1981.
- Morgan, W. J., Hotspot tracks and the early rifting of the Atlantic, *Tectonophysics*, 94, 123–139, 1983.
- O'Connor, J. M., Hotspots and the opening of the South Atlantic Ocean basin, Ph.D. thesis, Oreg. State Univ., Corvallis, 1990.
- O'Connor, J. M., and R. A. Duncan, Evolution of the Walvis Ridge and Rio Grande Rise hotspot system: Implications for African and South American plate motions over plumes, *J. Geophys. Res.*, 95, 17,475–17,502, 1990.
- Olson, P., and I. S. Nam, Formation of seafloor swells by mantle plumes, *J. Geophys. Res.*, 91, 7181–7191, 1986.
- Olson, P., and H. A. Singer, Creeping plumes, *J. Fluid Mech.*, 158, 511–531, 1985.
- Olson, P., G. Schubert, C. Anderson, and P. Goldman, Plume formation and lithosphere erosion: A comparison of laboratory and numerical experiments, *J. Geophys. Res.*, 93, 15,065–15,084, 1988.
- Patriat, P., Reconstitution de l'évolution du système de dorsales de l'Océan Indien par les méthodes de la cinématique des plaques, Ph.D. thesis, 308 pp., Univ. de Paris VII, 1983.
- Piccirillo, E. M., G. Bellieni, P. Comin-Chiaromonte, M. Ernesto, A. J. Melfi, I. G. Pacca, and N. Ussami, Significance of the Parana flood volcanism in the disruption of western Gondwanaland, in *The Mesozoic Flood Volcanism of the Parana Basin*, edited by E. M. Piccirillo, Inst. Astron. e Geof., Univ. de Sao Paulo, Sao Paulo, Brazil, 1988a.
- Piccirillo, E. M., A. J. Melfi, P. Comin-Chiaromonte, G. Bellieni, M. Ernesto, I. S. Marques, A. J. R. Nardy, I. G. Pacca, A. Roisenberg, and D. Stolfa, Continental flood volcanism from the Parana basin (Brazil), in *Continental Flood Basalts*, edited by J. D. Macdougall, pp. 195–238, Kluwer Academic, Dordrecht, Netherlands, 1988b.
- Pollitz, F. F., Episodic North America and Pacific plate motions, *Tectonics*, 7, 711–726, 1988.
- Rampino, M. R., and R. B. Stothers, Flood basalt volcanism during the last 250 million years, *Science*, 241, 663–667, 1988.

- Rea, D. K., and R. A. Duncan, North Pacific plate convergence: A quantitative record of the past 140 m.y., *Geology*, *14*, 373–376, 1986.
- Richards, M. A., Hotspots and the case against a uniform viscosity composition mantle, in *Glacial Isostasy, Sea-Level and Mantle Rheology*, edited by R. Sabadini and K. Lambeck, Kluwer Academic, Dordrecht, in press, 1991.
- Richards, M. A., and R. W. Griffiths, Deflection of plumes by mantle shear flow: Experimental results and a simple theory, *Geophys. J. R. Astron. Soc.*, *94*, 367–376, 1988.
- Richards, M. A., and R. W. Griffiths, Thermal entrainment by deflected mantle plumes, *Nature*, *342*, 900–902, 1989.
- Richards, M. A., and B. H. Hager, The Earth's geoid and the large-scale structure of mantle convection, in *The Physics of Planets*, edited by S. K. Runcorn, pp. 247–272, John Wiley, New York, 1988.
- Richards, M. A., R. A. Duncan, and V. E. Courtillot, Flood basalts and hotspot tracks: Plume heads and tails, *Science*, *246*, 103–107, 1989.
- Rona, P. A., and E. S. Richardson, Early Cenozoic global plate reorganization, *Earth Planet. Sci. Lett.*, *40*, 1–11, 1978.
- Royer, J.-Y., Evidence for the occurrence since 20 Ma of an additional plate boundary within the Central Indian basin (Indian Ocean) from plate tectonic reconstructions, *Eos Trans. AGU*, *69*, 1416, 1988.
- Royer, J.-Y., and D. T. Sandwell, Evolution of the Eastern Indian Ocean since the Late Cretaceous: Constraints from Geosat altimetry, *J. Geophys. Res.*, *94*, 13,755–13,782, 1989.
- Runcorn, S. K., A symposium on continental drift, I, Palaeomagnetic comparisons between Europe and North America, *Philos. Trans. R. Soc. London, Ser. A*, *258*, 1–11, 1965.
- Skilbeck, J. N., and J. A. Whitehead, formation of discrete islands in linear chains, *Nature*, *272*, 499–501, 1978.
- Sleep, N. H., Hotspots and mantle plumes: Some phenomenology, *J. Geophys. Res.*, *95*, 6715–6730, 1990.
- Stein, C. A., S. Cloetingh, and R. Wortel, Kinematics and mechanics of the Indian Ocean diffuse plate boundary zone, *Proc. Ocean Drill. Program Sci. Results*, *116*, 261–278, 1990.
- Stock, J. M., and P. Molnar, Uncertainties in the positions of the Australia, Antarctica, Lord Howe, and Pacific plates since the Late Cretaceous, *J. Geophys. Res.*, *87*, 4697–4714, 1982.
- Stock, J., and P. Molnar, Revised history of early Tertiary plate motion in the south-west Pacific, *Nature*, *325*, 495–499, 1987.
- Tucholke, B. E., and N. C. Smoot, Evidence for age and evolution of Corner Seamounts and Great Meteor Seamount chain from multibeam bathymetry, *J. Geophys. Res.*, *95*, 17,555–17,569, 1990.
- Turcotte, D. L., and G. Schubert, *Geodynamics: Applications of Continuum Physics to Geological Problems*, 450 pp., John Wiley, New York, 1982.
- Verplanck, E. P., and R. A. Duncan, Temporal variations in plate convergence and eruption rates in the western Cascades, Oregon, *Tectonics*, *6*, 197–209, 1987.
- Vink, G. E., A hotspot model for Iceland and the Vøring Plateau, *J. Geophys. Res.*, *89*, 9949–9959, 1984.
- Vogt, P. R., and J. R. Conolly, Tasmantid Guyots, the age of the Tasman Basin, and motion between the Australia plate and the mantle, *Geol. Soc. Am. Bull.*, *82*, 2577–2584, 1971.
- Watts, D. R., and A. M. Bramall, Palaeomagnetic evidence for a displaced terrain in Western Antarctica, *Nature*, *293*, 638–641, 1981.
- Wellman, P., and I. McDougall, Cainozoic igneous activity in eastern Australia, *Tectonophysics*, *23*, 49–65, 1974.
- Wells, R. E., D. C. Engebretson, P. D. Snavely, Jr., and R. S. Coe, Cenozoic plate motions and the volcano-tectonic evolution of western Oregon and Washington, *Tectonics*, *3*, 275–294, 1984.
- White, R., and D. McKenzie, Magmatism at rift zones: The generation of volcanic continental margins and flood basalts, *J. Geophys. Res.*, *94*, 7685–7729, 1989.
- White, R. S., G. D. Spence, S. R. Fowler, D. P. McKenzie, G. K. Westbrook, and A. N. Bowen, Magmatism at rifted continental margins, *Nature*, *330*, 439–444, 1987.
- Whitehead, J. A., Instabilities of fluid conduits in a flowing Earth—Are plates lubricated by the asthenosphere?, *Geophys. J. R. Astron. Soc.*, *70*, 415–433, 1982.
- Whitehead, J. A., and D. S. Luther, Dynamics of laboratory diapir and plume models, *J. Geophys. Res.*, *80*, 705–717, 1975.
- Wilson, J. T., A possible origin of the Hawaiian Islands, *Can. J. Phys.*, *41*, 863–868, 1963.
- Wilson, J. T., Evidence from ocean islands suggesting movement in the Earth, *Philos. Trans. R. Soc. London, Ser. A*, *258*, 145–165, 1965.
- Wyllie, P. J., Mantle fluid compositions buffered by carbonates in peridotite-CO<sub>2</sub>-H<sub>2</sub>O, *J. Geol.*, *85*, 187–207, 1977.
- Zindler, A., and S. Hart, Chemical geodynamics, *Annu. Rev. Earth Planet. Sci.*, *14*, 493–571, 1986.

---

R. A. Duncan, College of Oceanography, Oregon State University, Corvallis, OR 97331.

M. A. Richards, Department of Geology, University of California, Berkeley, CA 94720.